Available online at www.sciencedirect.com
ScienceDirect
Geochimica et Cosmochimica Acta 70 (2006) 5336–5355
Geochimica
www.elsevier.com/locate/gca

Microbial methane turnover at mud volcanoes of the Gulf of Cadiz

H. Niemann [a,b,*], J. Duarte [c], C. Hensen [d], E. Omoregie [a,g], V.H. Magalhães [c,e], M. Elvert [f], L.M. Pinheiro [c], A. Kopf [f], A. Boetius [a,g]

[a] Max Planck Institute for Marine Microbiology Bremen, Celsiusstr.1, 28359 Bremen, Germany
[b] Alfred Wegener Institute for Polar and Marine Research, 27515 Bremerhaven, Germany
[c] Geosciences Department and CESAM, University of Aveiro, Campus de Santiago, 3810-193 Aveiro, Portugal
[d] Leibniz Institute of Marine Sciences, IfM-GEOMAR, 24148 Kiel, Germany
[e] Department National Institute of Engineering, Technology and Innovation, Alfragide, 2720-866 Amadora, Portugal
[f] Research Center Ocean Margins, University of Bremen, 28359 Bremen, Germany
[g] International University Bremen, 28759 Bremen, Germany

Received 1 August 2005; accepted in revised form 3 August 2006

Abstract

The Gulf of Cadiz is a tectonically active area of the European continental margin and characterised by a high abundance of mud volcanoes, diapirs, pockmarks and carbonate chimneys. During the R/V SONNE expedition "GAP–Gibraltar Arc Processes (SO-175)" in December 2003, several mud volcanoes were surveyed for gas seepage and associated microbial methane turnover. Pore water analyses and methane oxidation measurements on sediment cores recovered from the centres of the mud volcanoes Captain Arutyunov, Bonjardim, Ginsburg, Gemini and a newly discovered, mud volcano-like structure called "No Name" show that thermogenic methane and associated higher hydrocarbons rising from deeper sediment strata are completely consumed within the seabed. The presence of a distinct sulphate–methane transition zone (SMT) overlapping with high sulphide concentrations suggests that methane oxidation is mediated under anaerobic conditions with sulphate as the electron acceptor. Anaerobic oxidation of methane (AOM) and sulphate reduction (SR) rates show maxima at the SMT, which was found between 20 and 200 cm below seafloor at the different mud volcanoes. In comparison to other methane seeps, AOM activity (<383 mmol m^{-2} $year^{-1}$) and diffusive methane fluxes (<321 mmol m^{-2} $year^{-1}$) in mud volcano sediments of the Gulf of Cadiz are low to mid range. Corresponding lipid biomarker and 16S rDNA clone library analysis give evidence that AOM is mediated by a mixed community of anaerobic methanotrophic archaea and associated sulphate reducing bacteria (SRB) in the studied mud volcanoes. Little is known about the variability of methane fluxes in this environment. Carbonate crusts littering the seafloor of mud volcanoes in the northern part of the Gulf of Cadiz had strongly ^{13}C-depleted lipid signatures indicative of higher seepage activities in the past. However, actual seafloor video observations showed only scarce traces of methane seepage and associated biological processes at the seafloor. No active fluid or free gas escape to the hydrosphere was observed visually at any of the surveyed mud volcanoes, and biogeochemical measurements indicate a complete methane consumption in the seafloor. Our observations suggest that the emission of methane to the hydrosphere from the mud volcano structures studied here may be insignificant at present.

1. Introduction

Constraining global sources and sinks of the greenhouse gas methane, and understanding the climate change coupled to variations in atmospheric methane, are important rationales of current biogeochemical research. Anthropogenic sources as well as natural emission from wetlands contribute significantly to the global emission of methane to the atmosphere, but the role of the ocean in global methane fluxes is not well understood (Reeburgh, 1996; Judd et al., 2002). Recently, marine mud volcanism has been identified as an important escape pathway for methane

* Corresponding author. Fax: +49 421 2028690.
E-mail address: hniemann@mpi-bremen.de (H. Niemann).

0016-7037/$ - see front matter © 2006 Elsevier Inc. All rights reserved.
doi:10.1016/j.gca.2006.08.010

and higher hydrocarbons (Dimitrov, 2002; Judd et al., 2002; Dimitrov, 2003). Mud volcanism is caused by various geological processes at continental margins such as tectonic accretion and faulting, rapid burial of sediments and emission of gases and fluids. Such processes may lead to high pore fluid pressures and sediment instabilities, and consequently cause mud extrusions. Since subsurface muds and shales of productive continental margins often contain methane and other hydrocarbons of thermogenic and/or microbial origin, mud flows can be accompanied by gas expulsion (Milkov, 2000; Kopf, 2002; Charlou et al., 2003; Somoza et al., 2003). Mud volcanoes (MVs) are structurally diverse, ranging in shape from amorphous mud pies to conical structures, and in size from a few metres to kilometres in diametre, attaining heights of up to a few 100 m (Dimitrov, 2002; Kopf, 2002). While there are only 650–900 known terrestrial mud volcanoes (Kopf, 2003), global estimates for marine mud volcanoes range between 800 and 100,000 (Milkov, 2000; Dimitrov, 2002, 2003; Kopf, 2003; Milkov et al., 2003). It is unknown how many of these submarine mud volcanoes are actively emitting methane to the hydrosphere. As a result, global estimates of methane emissions from these structures vary considerably. Recent estimates suggest that terrestrial and shallow water mud volcanoes contribute between 2.2 and 6 Tg year^{-1} of methane to the atmosphere (Dimitrov, 2003; Milkov et al., 2003) and that 27 Tg year^{-1} of methane may escape from deep water mud volcanoes (Milkov et al., 2003). Revised estimates of the total methane emission from MVs ranges between 35 and 45 Tg year^{-1} (Etiope and Milkov, 2004), 30 and 70 Tg year^{-1} (Etiope and Klusman, 2002), and—when using only known MVs and correcting for size of the edifice—between 0.3 (Kopf, 2003) and 1.4 Tg year^{-1} (Kopf, 2002). Clearly, a better understanding of mud volcano activity and methane turnover at these structures is needed, to evaluate the contribution of mud volcanism to the total annual methane emission to the atmosphere (535 Tg year^{-1}, Judd et al., 2002).

The main sink for methane in the ocean is the anaerobic oxidation of methane (AOM) with sulphate as the terminal electron acceptor (Barnes and Goldberg, 1976; Reeburgh, 1976; Iversen and Jørgensen, 1985; Hinrichs and Boetius, 2002; Nauhaus et al., 2002; Treude et al., 2003). This process is mediated by archaea, operating most likely in cooperation with sulphate reducing bacteria (SRB) (Hinrichs et al., 1999; Boetius et al., 2000; Orphan et al., 2001). So far, two groups of anaerobic methanotrophic archaea (ANME-1, ANME-2) have been identified (Hinrichs et al., 1999; Boetius et al., 2000; Orphan et al., 2001; Michaelis et al., 2002; Knittel et al., 2005). They usually occur together with SRB from a distinct, yet uncultivated cluster within the *Desulfosarcina/Desulfococcus* group (Seep-SRB1; Knittel et al., 2003). Generally, microbial methane oxidation is characterised by a strong discrimination against the heavy, stable carbon isotope ^{13}C, leading to a significant depletion in the ^{13}C-content of metabolites and biomass (Reeburgh and Heggie, 1977; Whiticar et al., 1986; Summons et al., 1994; Elvert et al., 1999; Thiel et al., 1999; Whiticar, 1999; Orphan et al., 2001). Such conspicuous isotope signatures of lipid biomarkers for the archaeal and bacterial partners in AOM mediating communities have been a main tool in studying the diversity and functioning of cold seep ecosystems (Hinrichs et al., 1999; Pancost et al., 2000; Elvert et al., 2001; Orphan et al., 2001; Michaelis et al., 2002; Elvert et al., 2003; Blumenberg et al., 2004; Elvert et al., 2005; Niemann et al., 2005). Active mud volcanoes in the Mediterranean Sea, e.g. Napoli, Amsterdam and Kazan (Pancost et al., 2000; Aloisi et al., 2002; Haese et al., 2003; Werne et al., 2004); the Black Sea, e.g. Dvurechenskii and Odessa (Bohrmann et al., 2003; Stadnitskaia et al., 2005); and the Barents Sea, e.g. Håkon Mosby (Vogt et al., 1997a,b; Damm and Budéus, 2003; De Beer et al., 2006) are characterised by steep gradients of pore water solutes due to upward fluid and gas flow and high rates of AOM and sulphate reduction (SR). Several of these geo-bio-systems were also found to support enormous biomasses of chemosynthetic symbiotic tubeworms and bivalves, which are fuelled by methane and/or sulphide, and mats of giant sulphide oxidising bacteria, (Southward et al., 1981; Fisher, 1990; Olu et al., 1997a; Gebruk et al., 2003).

During the UNESCO program "Training through Research (TTR)" with R/V Prof. Logachev, numerous mud volcanoes hosting methane-hydrate were discovered in the Gulf of Cadiz (Kenyon et al., 2000; Gardner, 2001; Kenyon et al., 2001; Mazurenko et al., 2002; Somoza et al., 2002; Pinheiro et al., 2003). However, the geochemical and microbiological activity of these potential seep structures and the occurrence of methane emission to the hydrosphere remained unknown. As part of the Gibraltar Arch Project (GAP), we studied several mud volcanoes with the aid of seafloor video imaging as well as video-guided sampling of sediments and carbonate crusts during a cruise with R/V Sonne in 2003 (SO-175). The main goals of this investigation were to survey the occurrence of methane seepage at mud volcanoes in the Gulf of Cadiz, to compare the distribution and magnitude of AOM by rate measurements and diffusive flux calculations, as well as to identify the key methanotrophs using lipid biomarker and 16S rDNA methods.

2. Materials and methods

2.1. Geological setting and videographic observations

The Gulf of Cadiz is located west of the Gibraltar Arc, between Iberia and the African plate (Fig. 1). This area has experienced a complex tectonic history with several episodes of extension, strike-slip and compression related to the closure of the Tethys Ocean, the opening of the N-Atlantic, and the African–Eurasian convergence since the Cenozoic (Maldonado et al., 1999). During the Tortonian, a large olistrostome body made of eroded material from

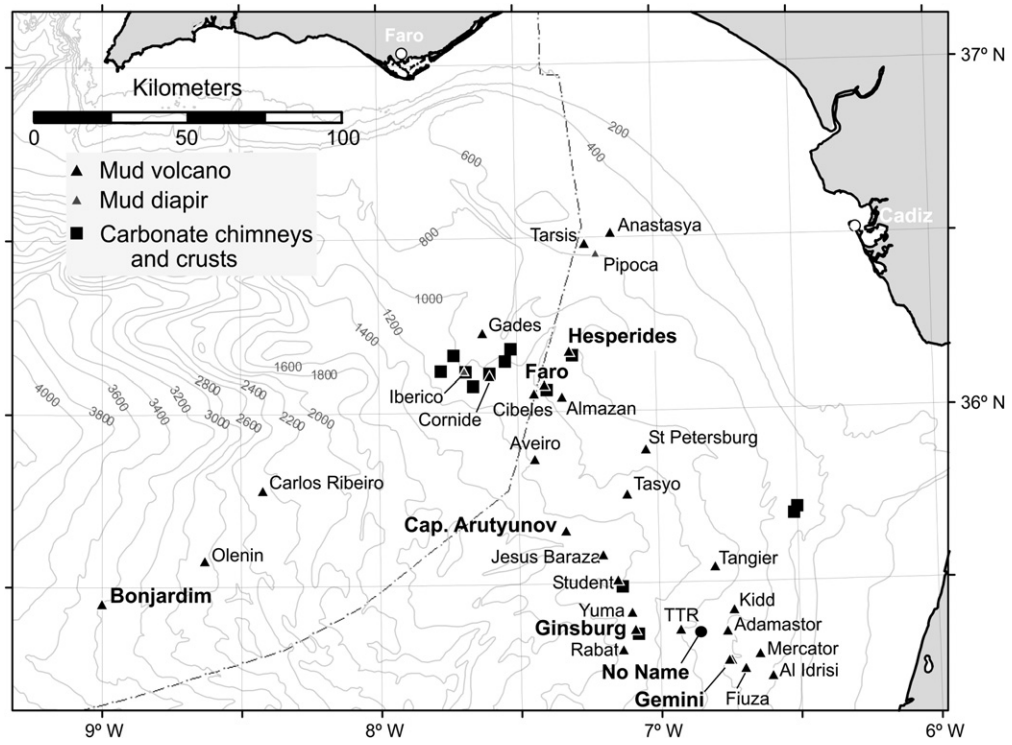

Fig. 1. Bathymetric chart of the Gulf of Cadiz showing the locations of known mud volcanoes, diapirs and areas where carbonate chimneys and crusts were discovered. The structures studied during the SO-175 expedition are in bold face letters.

the Betic Cordillera (Spain) and Rif Massif (Morocco) was emplaced west of the Straits of Gibraltar (Maldonado and Comas, 1992; Somoza et al., 2003). Due to the ongoing compression, these rapidly deposited sediments dewater intensely and form MVs and fluid escape structures (Diaz-Del-Rio et al., 2003). The Gulf of Cadiz has been intensely surveyed with geophysical tools, leading to the discovery of the first MVs, mud diapirs and pockmarks in 1999 (Kenyon et al., 2000; Gardner, 2001; Pinheiro et al., 2003). In addition, an extensive field of mud volcanoes and diapiric structures covered with carbonate chimneys and crusts was discovered along or in close proximity of the main channels of the Mediterranean outflow water (Kenyon et al., 2000, 2001; Diaz-Del-Rio et al., 2003; Somoza et al., 2003; Kopf et al., 2004).

In the present study, Captain Arutyunov (Capt. Arutyunov), Bonjardim, Ginsburg, Gemini, Hesperides and Faro MV and a newly discovered structure termed ''No Name'', were investigated (Fig. 1, Table 1). Prior to biogeochemical sampling, a few transects across the selected MVs were surveyed with the video-sled Ocean Floor Observation System (OFOS), or with a video-guided multiple-corer (MUC, Table 1). Both systems are equipped with powerful lamps and a video camera. Video observations were made from a vertical perspective at ca. 1–2 m above the sea bottom to monitor an area of approximately 1 m^2. The systems were passively towed at minimum speed (<1.84 km h^{-1}) along 2–3 transects of 1–3 km crossing the rim and apex of the edifices with a total bottom observation time of approximately 8 h per mud volcano (Table 1, Kopf et al., 2004). The video-guided MUC was also used to select representative sampling positions and to retrieve undisturbed surface sediments (next section).

2.2. Sample collection and storage

Sediments from several mud volcanoes were sampled by gravity coring in the central crater region (Table 1, Fig. 2), retrieving up to 5 m of sediment. Additionally, surface sediments of Capt. Arutyunov and Bonjardim MV were obtained with a video-guided MUC because the top decimetres of sediment cover are often lost during gravity core retrieval. Video-guided MUC sampling enabled the retrieval of undisturbed surface sediments of up to 50 cm sediment depth. With this method, the seafloor can be observed when the MUC is towed at minimum speed at about 1–2 m above bottom. The MUC is launched immediately when targeted seafloor structures are observed. Compared to the gravity core, MUC-cores contained a broader horizon of hemipelagic surface sediments providing further evidence for a loss of surface sediments during gravity coring. To account for this loss, we aligned the depth of gravity cores obtained from Capt. Arutyunov and Bonjardim MV according to the vertical sulphate profiles of MUC-cores recovered from one site, assuming that sulphate concentrations are mainly a function of depth in proximate cores. According to this procedure, the top of the gravity cores recovered from Capt. Arutyunov and Bonjardim

Table 1
Mud volcanoes investigated during the cruise SO-175

Structure	Relief [m]	Diam. [km]	Water depth [m]	Device	Core/Grab	Lat. N	Long. W	Applied methods
CAMV	80	2.0	1315	MUC	GeoB 9036-2	35° 39.72′	07° 19.98′	V, CH_4, SO_4^{2-}, C_{2+}, H_2S, F, R, L, D
				GC	GeoB 9041-1	35° 39.70′	07° 19.97′	CH_4, SO_4^{2-}, C_{2+}, H_2S
Bonjardim	100	1.0	3090	MUC	GeoB 9051-1	35° 27.72′	08° 59.98′	V, CH_4, SO_4^{2-}, C_{2+}, H_2S, R, L
				GC	GeoB 9051-2	35° 27.61′	09° 00.03′	CH_4, SO_4^{2-}, C_{2+}, H_2S, F, R, L
Ginsburg	150	4.0	910	GC	GeoB 9061-1	35° 22.42′	07° 05.29′	V, CH_4, SO_4^{2-}, H_2S, F
Gemini	200	4.9	435	GC	GeoB 9067-1	35° 16.92′	06° 45.47′	CH_4, SO_4^{2-}, H_2S, F
No Name	150	3.7	460	GC	GeoB 9063-1	35° 21.99′	06° 51.92′	CH_4, SO_4^{2-}, H_2S, F
Hesperides	160	3.0	690	Grab	GeoB 9023-1	36° 10.73′	07° 18.39′	V, L
Faro	190	2.6	810	Grab	GeoB 9029-3	36° 05.68′	07° 24.12′	V, L

The water depth refers to the highest elevation of the mud volcanoes. V, video observations; CH_4, methane concentration measurements; SO_4^{2-}, sulphate concentration measurements; C_{2+}, concentration measurements of higher hydrocarbons; F, diffusive methane and sulphate flux calculation; R, AOM and SR rate measurements; L, lipid analyses; D, DNA analysis.

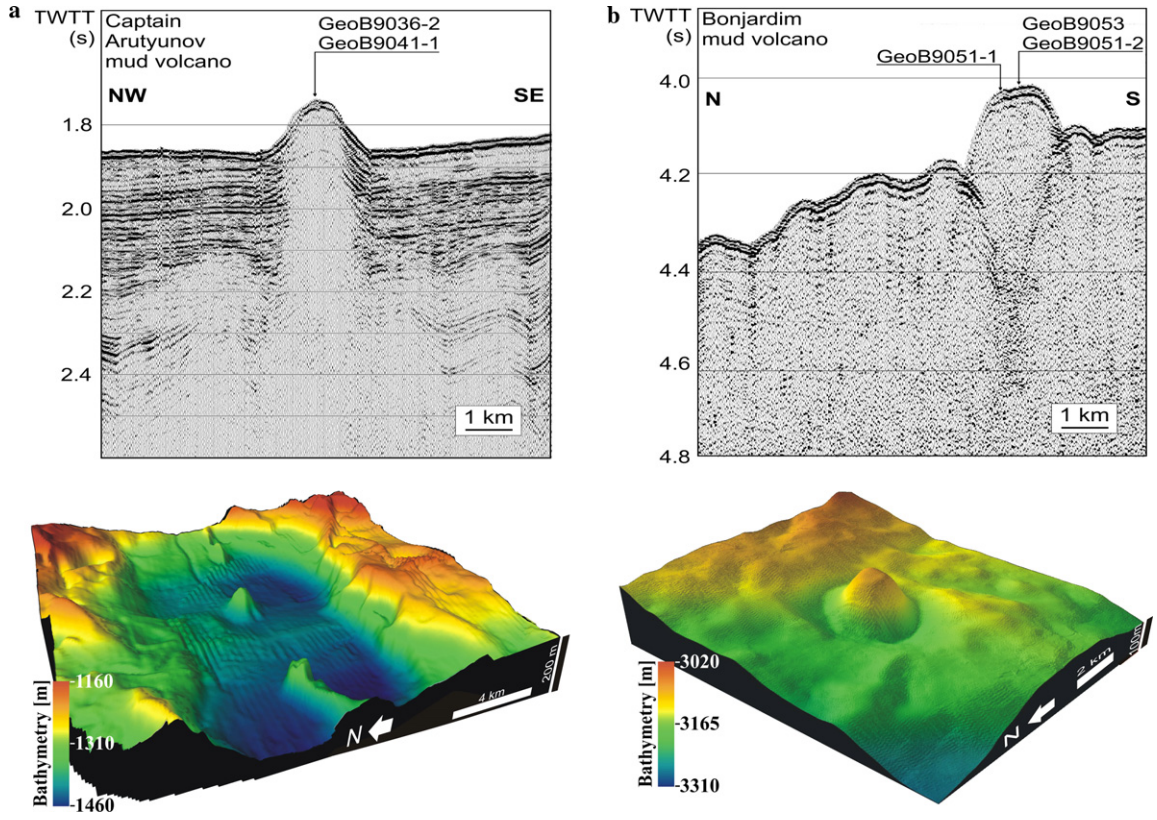

Fig. 2. Seismic images and 3D images of multibeam bathymetry of Captain Arutyunov (a) and Bonjardim mud volcano (b). Seismic images show the central conduit below the mud volcanoes and sampling position of the cores recovered during the SO-175 expedition. Captain Arutyunov and Bonjardim MV are conical shaped structures with a relief of 80 and 100 m and a diametre of ca. 2 and 1 km, respectively. Colours denote the bathymetry (m below sea surface). Seismic images were modified after Kenyon et al. (2001) (a) and Pinheiro et al. (2003) (b).

MV were from 40 to 12.5 cm sediment depth, respectively. Aligning proximate core sections is an approach to account for a loss of an unknown quantity of surface sediments during gravity coring. However, this can be problematic if the spatial variability of geochemical gradients is high.

Upon recovery, gravity cores were sectioned into 1 m pieces, which were cut longitudinally into halves, just before sub sampling. All cores were immediately transferred into a cold room and subsampled for concentration measurements of pore water constituents (methane, sulphate, sulphide), AOM and SR rate measurements as well as for lipid biomarker and 16S rDNA analyses (Table 1). Sediments for measurements of methane and sulphate concentrations and turnover rate measurements were subsampled vertically with push cores (acrylic core liners, 26 mm diametre, $n = 3$) from MUC-cores (Jørgensen, 1978; Treude et al., 2003). Gravity cores were subsampled by plugging

glass tubes (60 mm length, 10 mm diametre, $n = 5$) into selected ca. 10 cm wide sediment horizons (every 20–30 cm). The tubes were then sealed with butyl rubber stoppers to prevent gas loss during the anaerobic incubation. Sediment samples for pore water extraction, biomarker and 16S rDNA analyses were collected from 2 cm sections of MUC-cores and from ca. 10 cm wide sediment horizons (every 20–30 cm) of gravity core sections. Directly after subsampling, pore water from these sediment horizons was extracted by pressure filtration (5 bars) through Teflon squeezers provided with 0.2 μm cellulose acetate filters according to previous works (Reeburgh, 1967; Niewöhner et al., 1998; Hensen et al., 2003). Subsequently, the pore water was immediately fixed (next section). Lipid and DNA samples were stored in cleaned glass vials at −20 °C until extraction in the home laboratory. Carbonate crusts from Hesperides and Faro MV were collected with a video-guided grab-sampler (Table 1). Because Hesperides MV consist of six individual cones, the grab sample was taken from the apex of the highest (north-eastern) summit. The grab-sampler allows to retrieve samples down to a depth of ca. 0.5 m below seafloor (bsf). The videographic observation and sampling procedure is similar to the technique used for video-guided coring as explained above. Upon recovery, carbonate crusts for lipid biomarker analyses were transferred into plastic bags and stored at −20 °C until extraction.

2.3. Methane concentrations

Methane concentrations in sediments were determined according to the ''head space'' method from 5 ml sediment fixed with 10 ml NaOH (2.5%, w/v) in glass vials (20 ml) as described previously by Treude and co-workers (2003). A vertical resolution of 2 cm was chosen for surface samples from MUC-cores, and of 20–30 cm for subsurface samples from gravity cores. The concentrations presented here are *ex situ* methane concentrations. As a result of depressurisation and warming of the core during sediment retrieval, concentrations above 1.4 mM (saturation at 1 bar and 4 °C) would have led to degassing during retrieval and sediment subsampling. Also, dissociation of gas hydrates upon recovery may lead to biased methane concentrations in the cores. We tried to minimise the problem by (a) subsampling immediately after opening the core, and (b) subsampling of deeper sediments below the longitudinal opening plane of the gravity core with glass syringes. Methane concentrations were determined shortly after the cruise (<2 month) from 200 μl aliquots of the head space using a gas chromatograph (5890A, Hewlett Packard) equipped with a packed stainless steal Porapak-Q column (6 ft., 0.125 in, 80/100 mesh, Agilent Technologies) and a flame ionisation detector (Treude et al., 2003). The carrier gas was helium at a flow rate of 30 ml min^{-1}. The column temperature was 40 °C. The chromatography system was calibrated for a concentration range of 0.001–5 mM methane (final concentration in the sediment). Sediment samples from Capt. Arutyunov and Bonjardim MV were additionally analysed for the concentrations of the higher hydrocarbons (C_{2+}) ethane, propane, isobutene and butane (Σbutane) using the above-described chromatography setting with a temperature gradient. Subsequent to injection at 40 °C, the temperature was increased at a rate of 2 °C min^{-1} to 200 °C and held for 20 min. Identity and concentrations of methane and C_{2+}-compounds were determined with standards of known hydrocarbon compositions.

2.4. Sulphate and sulphide concentrations

Sulphate and sulphide concentrations were analysed according to modified methods from Cline (1969) and Small et al. (1975), respectively, as described elsewhere (Grasshoff et al., 1983). Briefly, sulphide concentrations were determined immediately after pore water squeezing by adding 1 ml of pore water to 50 μl of a zinc acetate gelatine solution. Zinc acetate gelatine solution consists of 50 mg gelatine and 261 mg ZnAc dissolved in 25 ml O_2-free water. Sulphide was quantitatively removed as ZnS and kept in colloidal solution. After adding 10μl of 4% *N*,*N*-dimethyl-1,4-phenylenediamine-dihydrochloride dissolved in 6 N HCl (w/v), the concentration was determined photometrically by measuring the absorbance after 1 h at 670 nm. Sulphate concentrations were determined on 2 ml subsamples of filtered pore water using a Sykam-S ion chromatography system equipped with an anion exchange column (LCA A14). 7.5 mM Na_2CO_3-solution was used as an eluent at a flow rate of 1.75 ml min^{-1}. Samples were diluted by 1:54 with the eluent prior to injection. Sulphate concentrations were determined with a Sykam S3110 conductivity detector.

2.5. Diffusive flux calculations

Diffusive fluxes were calculated to compare areal rates of AOM and SR, to estimate the activity of Ginsburg and Gemini mud volcano as well as the No Name structure and to compare the surveyed systems to other seeps in the world oceans. This approach bears several problems, namely potential artefacts in the *ex situ* concentrations of porewater species due to degassing, the assumption of steady state in the porewater system, and the alignment of sediment cores. At Bonjardim mud volcano, the alignment of pore water profiles was discontinuous, while the resolution of pore water gradients was not well resolved at Ginsburg and Gemini mud volcano. Where possible, we determined two concentration gradients: one from the aligned profile and the other from the profile of the gravity core in order to provide a possible range of the sulphate and sulphide fluxes.

Local fluxes (J) were calculated from the vertical profiles of pore water constituents (methane, sulphate, sulphide) according to Fick's first law of diffusion assuming steady state conditions (e.g. Niewöhner et al., 1998; Berner, 1980 and references therein):

$$J = -\phi D_s \frac{\delta C}{\delta x} \quad (1)$$

where D_s is the diffusion coefficient in the sediments (in $cm^2\ year^{-1}$), ϕ the porosity (in %) and $\frac{\delta C}{\delta x}$ the local concentration gradient (in cm^{-4}). $\frac{\delta C}{\delta x}$ was determined from the depth intervals where the concentration change was maximal. D_s was determined from the molecular diffusion coefficient after Boudreau (1997)

$$D_s = \frac{D_0}{1 - \ln(\phi)^2} \quad (2)$$

For each mud volcano, D_0 values were corrected for temperature (3–12 °C, depending on the actual bottom water temperature), resulting in values ranging between 291 to 392, 178 to 244 and 356 to 434 for methane, sulphate and sulphide, respectively (Boudreau, 1997). ϕ was determined from the weight loss per volume of wet sediment after drying to stable weight at 60 °C. In general, ϕ decreased with depth showing values of 57–76% in the top sections and 51–60% in the bottom sections of the retrieved MUC- and GC-cores (data shown for the SMT, Table 2).

2.6. Ex situ AOM and SR rate measurements

Sediment for turnover rate measurements recovered from Capt. Arutyunov and Bonjardim MV were incubated on board according to previously described methods (Jørgensen, 1978; Treude et al., 2003; Treude et al., 2005). Briefly, 25 µl $^{14}CH_4$ (dissolved in water, 2.5 kBq) or 5 µl $^{35}SO_4^{2-}$ tracer (dissolved in water, 50 kBq) were injected into butyl rubber sealed glass tubes from gravity core subsampling, and in 1 cm intervals into small push cores (whole core injection) used for MUC-core subsampling. Incubations were carried out for 24 h at *in situ* temperature in the dark. Subsequently, incubated AOM and SR rate samples were fixed in 25 ml NaOH (2.5%, w/v) and 25 ml zinc acetate solution (20%, w/v), respectively. Further processing of AOM and SR rate samples was performed according to Treude et al. (2003) and references therein. Turnover rates were calculated according to the following formulas:

$$\mathrm{AOM} = \frac{^{14}CO_2}{^{14}CH_4 + ^{14}CO_2} \times \frac{\text{conc. } CH_4}{\text{incubat. Time}} \quad (3)$$

$$\mathrm{SRR} = \frac{\mathrm{TRI}^{35}S}{^{35}SO_4^{2-} + \mathrm{TRI}^{35}S} \times \frac{\text{conc. } SO_4^{2-}}{\text{incubat. Time}} \quad (4)$$

Here, $^{14}CO_2$, $^{35}SO_4^{2-}$ and $TRI^{35}S$ are the activities (Bq) of carbon dioxide, sulphate and total reduced sulphur species, respectively, whereas conc. CH_4 and conc. SO_4^{2-} are the concentrations of methane and sulphate (per volume of fresh sediment) at the beginning of the incubation. To compare *ex situ* microbial rates with the diffusive fluxes of methane and sulphate, AOM and SR rates were integrated over depth (0–80 cm below seafloor) from the alignments of cores 9036-2 and 9041-4 as well as 9051-1 and 9051-2, respectively. *Ex situ* rate measurements may differ from *in situ* rates due to the effect of depressurisation on concentrations of gaseous and dissolved components.

2.7. Extraction of sediment and carbonate samples and preparation of derivates

Sediments from Capt. Arutyunov and Bonjardim MV as well as carbonate crusts from Hesperides and Faro MV were analysed for lipid biomarker signatures. The extraction procedure and preparation of fatty acid methyl esters (FAMES) was carried out according to previously described methods (Gillian et al., 1981; Elvert et al., 2003; Niemann et al., 2005). Briefly, total lipid extracts (TLE) were obtained from ca. 20 g of wet sediment and from authigenic carbonates disintegrated with HCL (2 M) prior to extraction. The TLE was extracted by subsequent ultrasonication using organic solvents of decreasing polarity (dichloromethane/methanol (1:2, v/v), dichloromethane/methanol (2:1 v/v), dichloromethane). Internal standards of known concentration and carbon isotopic compositions were added prior to extraction. Fatty acid moieties present in glyco and phospholipids were cleaved by saponification with methanolic KOH-solution. After extraction of the neutral lipid fraction from this mixture, fatty acids (FAs) were methylated with BF_3 in methanol yielding FAMES. Double bond positions of monoenoic FAs were determined

Table 2
Concentrations gradients, diffusive fluxes and *ex situ* AOM and SR rates integrated over depth

Structure	Core GeoB	Porosity [%]	Conc. gradient [µmol cm^{-4}]			Diffusive fluxes [mmol $m^{-2}\ year^{-1}$]			Microbial turnover [mmol $m^{-2}\ year^{-1}$]	
			CH_4	SO_4^{2-}	Sulphide	CH_4	ΣSO_4^{2-}	ΣSulphide	AOM	SR
Capt. Arutyunov	9036-2	56	0.40	−1.12	0.63	407	708	702	383	577
Bonjardim	9051-2	58	0.09	−0.76, −1.67*	0.23, 0.73* (−0.07)	76	388, 867‡	299, 795‡	36	690
Ginsburg	9061-1	60	0.05	−0.92 (0.35)	0.32 (−0.15)	55	852	565		
Gemini	9067-1	56	0.02	−0.61	0.12 (−0.09)	21	388	272		
No Name	9063-1	57	0.03	−0.11	0.04 (−0.06)	29	74	108		

A negative concentration gradient indicates downward directed flux; a positive value indicates upward flux. Flux values are given without algebraic signs. * and ‡ denote gradients and total sulphate fluxes determined from aligning multiple- and gravity cores. Gradients in brackets indicate upward diffusing sulphate and downward diffusing sulphide, respectively.

by analysis of dimethyl disulphide adducts according to methods described elsewhere (Nichols et al., 1986; Moss and Lambertfair, 1989).

Neutral lipids were further separated into hydrocarbons, ketones and alcohols on a SPE silica glass cartridge (0.5 g packing) with solvents of increasing polarity (*n*-hexane/dichloromethane (95:5, v/v), *n*-hexane/dichloromethane (2:1, v/v), dichloromethane/acetone (9:1, v/v)) (Niemann et al., 2005). Alcohols were derivatised with bis(trimethylsilyl)triflouracetamid (BSTFA) forming trimethylsilyl (TMS) ethers prior to analyses.

2.8. Gas chromatography

Concentrations of single lipid compounds were determined by gas chromatography analysis using a Varian 30 m apolar CP-Sil 8 CB fused silica capillary (0.25 mm internal diametre [ID], film thickness 0.25 μm) in a Hewlett Packard 6890 Series gas chromatograph equipped with an on column injector and a flame ionisation detector. Initial oven temperature was 80 °C. Subsequently to injection, the initial temperature was increased to 130 °C at a rate of 20 °C min^{-1}, then raised to 320 °C at a rate of 4 °C $min^{-1}$and held at 320 °C for 30 min. The carrier was helium at a constant flow of 2 ml min^{-1} and the detector temperature was set to 310 °C. Concentrations were calculated relative to internal standards present within the respective lipid fraction.

2.9. Gas chromatography-mass spectrometry (GC-MS), gas chromatography-isotope ratio mass spectrometry (GC-IRMS)

Identity and stable carbon isotope ratios of individual compounds were determined by GC-MS and GC-IRMS analysis, respectively. Instrument specifications and operation modes of the GC-MS and GC-IRMS units were set according to Elvert et al. (2003). Identities of acquired mass spectra were compared to known standards and published data. Stable isotope ratios are given in the δ-notation against Pee Dee Belemnite. $\delta^{13}C$-values of FAs and alcohols were corrected for the introduction of additional carbon atoms during derivatisation. Internal standards were used to monitor precision and reproducibility during measurements. Reported $\delta^{13}C$-values have an analytical error of ±1‰.

2.10. DNA extraction and clone library construction

Total community DNA was extracted from sediments (ca. 1 g) collected from the SMT of Capt. Arutyunov MV (30–40 cm) using the FastDNA spin kit for soil (Q-Biogene, Irvine, California, USA). Samples were bead-beat in a Fastprep machine (Q-Biogene, Irvine, California, USA) at speed 4.5 for 30 s. All other steps in the DNA extraction procedure were preformed according to the manufacturer's recommendations. Almost full-length archaeal and bacterial 16S rRNA genes were amplified from sediments samples using the primers 20f (Massana et al., 1997) and Uni1392R (Lane et al., 1985) for *Archaea* and GM3F (Muyzer et al., 1995) and GM4R (Kane et al., 1993) for *Bacteria*. Polymerase chain reactions (PCRs) were performed with TaKaRa Ex *Taq* (TaKaRa, Otsu Japan), using 2.5 U of enzyme, 1× Buffer, 4 mM of $MgCl_2$, 4 mM of each dNTP, 1 μM of each primer and 2 μl of template in a 50 μl reaction. PCRs were preformed in a Mastercycler machine (Eppendorf, Hamburg, Germany), with the following cycling conditions: 95 °C for 2 min, then 30 cycles of 95 °C for 30 s, 60 °C (*Archaea*) or 50 °C (*Bacteria*) for 30 s and 72 °C for 3 min, followed by a final incubation step at 72 °C for 10 min. PCR products were visualised on an agarose gel, and the 16S band excised. PCR products were purified using the QIAquick Gel Extraction Kit (Qiagen, Hilden, Germany). Two microliters of purified DNA were ligated in the pGEM T-Easy vector (Promega, Madison, WI) and transformed into competent E. coli TOP10 cells (Invitrogen, Carlsbad, CA) according to the manufacturer's recommendations. Transformation reactions were plated on LB-agarose plates. Overnight cultures were prepared from individual colonies picked from these plates using the Montage Plasmid Miniprep 96 kit (Millipore, Billerica, USA). Purified plasmids were sequenced in one direction, with either the 958R (*Archaea*) or GM1F (*Bacteria*) primers using the BigDye Terminator v3.0 Cycle Sequencing kit (Applied Biosystems, Foster City, USA). Samples were sequenced on an Applied Biosystems 3100 Genetic Analyser (Foster City, USA). A total of 39 archaeal and 47 bacterial clones were partially sequenced (~0.5 kb). Using the ARB software package, the sequences were calculated into existing phylogentic trees by parsimony without allowing a change in the tree topology. Representative sequences of each cluster were then fully sequenced (~1.3 kb) and matched against the NCBI database (http://www.ncbi.nlm.nih.gov/BLAST). Sequences were submitted to the Genbank database (http://www.ncbi.nlm.nih.gov/) and are accessible under the following Accession Nos.: DQ004661–DQ004676 and DQ004678–DQ004680.

3. Results

3.1. Field observations

A detailed description of seafloor video observations, sedimentology and sampling locations is provided in the cruise report of R/V SONNE expedition SO-175 (Kopf et al., 2004). The mud volcanoes Capt. Arutyunov, Bonjardim, Ginsburg, Gemini, and Faro studied here are cone shaped structures with a relief of up to 200 m and a maximum diametre of 4.9 km (Fig. 2a, b; Table 1). Hesperides MV has comparable dimensions but is composed of six individual cones. A new structure was discovered east of the TTR MV and termed "No Name" (Fig. 1). Video observations of the mud volcanoes Capt. Arutyunov, Bon-

jardim, Ginsburg, Hesperides, and Faro did not reveal indications for recent gas, fluid or mud expulsion during the transects across the central craters of each structure. The centres of Capt. Arutyunov, Bonjardim and Ginsburg MV were covered with light beige sediments (shown for Capt. Arutyunov MV, Fig. 3a). At Capt. Arutyunov MV, some sediment stretches were scattered with accretions, interpreted as mud clasts, which may indicate past mud eruptions (Fig. 3b). At Ginsburg MV, a few small carbonate crusts (<0.5 m) were observed on the seafloor. Beside these observations, no other distinctive geological or biological features indicating gas or fluid seepage were visible on video images at Ginsburg MV. Surface sediments recovered from Capt. Arutyunov MV contained very thin tubeworms (diametre <1 mm), which extended down to 20 cm into the sediment. These were not visible on video images due to their low abundance and small diametre. Tubeworms are regarded as indicator species for reduced environments because the known species harbour methane or sulphide oxidising symbionts, indicating sulphide and/or methane availability in the sediments (Southward et al., 1981, 1986; Schmaljohann and Flugel, 1987; Sibuet and Olu, 1998; Kimura et al., 2003; Southward et al., 2005). The central areas of Hesperides and Faro MV were littered with fragments of carbonate chimneys and carbonate crusts (shown for Hesperides MV, Fig. 3c). Both, chimneys and crusts were ranging in size from several centimetres to metres in length and diametre, respectively. At Faro MV, a few, small patches covered with microbial mats possibly consisting of filamentous sulphide oxidising bacteria were observed (Fig. 3d). Moreover, TV-guided grab samples recovered from this MV also contained a few specimens of the deep-dwelling chemosynthetic clam *Acharax* sp. usually harbouring sulphide oxidising bacteria in their gills (Felbeck, 1983; Krueger and Cavanaugh, 1997; Peek et al., 1998; Sibuet and Olu, 1998). Video observations were not carried out at Gemini MV and the "No Name" structure.

The MUC-cores retrieved from Capt. Arutyunov and Bonjardim MV contained yellowish, muddy sediments in the top sections from 0 to 20 and 0 to 40 cm bsf, respectively. The bottom sections of the MUC-cores contained mud breccia, a mud matrix with clasts extruded from greater depth below these edifices (Cita et al., 1981; Akhmanov and Woodside, 1998). The gravity cores retrieved from these MVs as well as those retrieved from Ginsburg and Gemini also contained mud breccia. The gravity core recovered from the "No Name" structure contained a matrix of cold water coral fragments and greyish mud but no mud breccia. Hence, the relation of the "No Name" geostructure to mud volcanism remains unknown. Grab samples from Hesperides and Faro MV contained carbonate fragments and mud breccia. After recovery, the temperature in the top sediment section (~1 m) at Bonjardim MV was ca. 3 °C. In contrast, the temperature was considerably higher at Capt. Arutyunov (12 °C), Ginsburg MV, Gemini MV and the "No Name" structure (10 °C, respectively) most probably as a result of the warm Mediterranean outflow water, which contributes to the bottom water at these MVs.

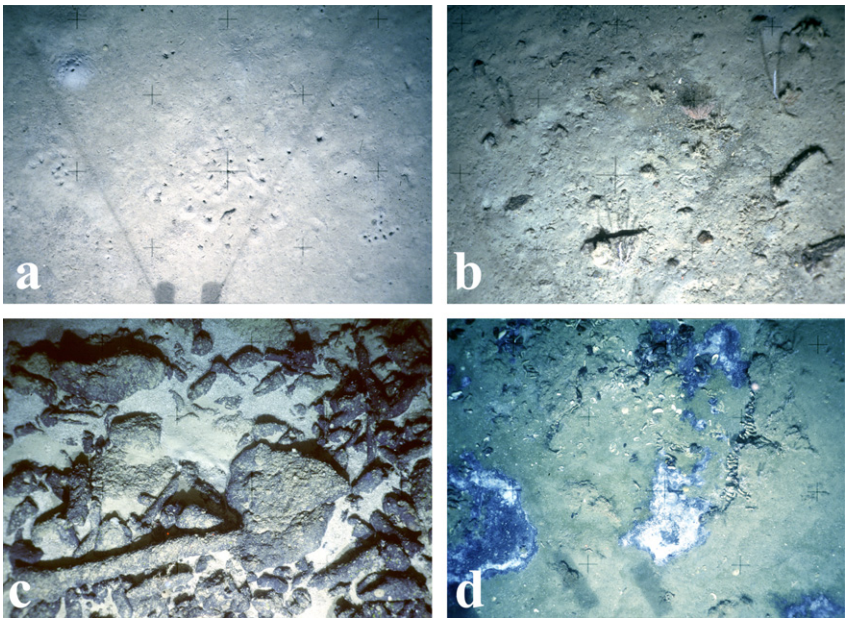

Fig. 3. Seafloor images (ca. 1 m^2) of Capt. Arutyunov (a,b), Hesperides (c) and Faro MV (d). The surface of Capt. Arutyunov, Bonjardim, Ginsburg MV were found to be covered by pelagic sediments as shown in (a). The holes are burrows of crabs. Some sediment stretches at Capt. Arutyunov MV contained accretions that are interpreted as clasts (b) indicating past mud flows. Hesperides and Faro mud volcano were littered with carbonate chimneys and crusts as shown for Hesperides MV in (c). At Faro mud volcano, also a few dark sediment patches probably covered with whitish, giant sulphide-oxidizing bacteria were observed (d).

3.2. Captain Arutyunov MV

3.2.1. Methane, C_{2+}, sulphate and sulphide

Methane concentrations in surface sediments (0–20 cm, Fig. 4a) were <0.001 mM indicating a complete consumption of methane rising from deeper sediment strata. A distinct SMT was observed in the lower half of the MUC-core section (25–40 cm bsf.) with *ex situ* methane concentrations above saturation at atmospheric pressure, and sulphate concentrations dropping below 0.5 mM. The steepest gradients of methane and sulphate found in this zone amounted to 0.4 and −1.12 μmol cm^{-4}, respectively (Fig. 4a, Table 2). Small gas hydrate chips were found throughout the whole gravity core section from 44 to 235 cm bsf (1941-1). Similar to methane, concentrations of C_{2+}-compounds decreased across the SMT (Fig. 4b). Hydrocarbons in the sediment comprised methane (>99%), ethane (<0.4%), propane (<0.07%) with trace amounts of butane and isobutene present indicating a thermogenic origin of these gases (Nuzzo et al., 2005; Stadnitskaia et al., 2006 and references therein). Sulphide concentrations peaked in the SMT with 4.8 mM at 39 cm bsf (Fig. 4d). The steepest sulphide gradient was 0.63 μmol cm^{-4} (Fig. 4d, Table 2). A downward sulphide gradient could not be determined because highest sulphide concentrations were observed in the lowest sediment horizon of the MUC-core at Capt. Arutyunov MV. Unfortunately, the sulphide profile could not be aligned with the gravity core section.

3.2.2. AOM, SR rates and diffusive fluxes

AOM and SR rates at Capt. Arutyunov MV were highest in the SMT at 39 cm bsf with maximum values of 11 and 25 nmol cm^{-3} d^{-1}, respectively (Fig. 4c). AOM and SR rates sharply decreased above and below this horizon. Replicate AOM and SR rate measurements showed a standard error of 33% and 37% of the average value, respectively. The areal integration resulted in 1.8 higher SR rates compared to AOM (Table 2). The areal AOM and SR rate were in good agreement with diffusive flux calculations showing a 1.7-fold higher sulphate flux compared to the methane flux. The sulphide flux to the surface (upward flux) was comparable to the total downward flux of sulphate (Table 2).

3.2.3. Lipid biomarker

Diagnostic archaeal and bacterial lipid concentrations were strongly increased in sediments at the SMT (Fig. 4e, g). Here, stable carbon isotope analysis revealed highest depletion in ^{13}C with minimum values of −92‰ (*sn2*-hydroxyarchaeol) in archaeal specific diether lipids and −82‰ ($cyC_{17:0\omega5,6}$) in bacterial specific FAs (Table 3, Fig. 4f, g) indicating the incorporation of methane derived carbon in archaeal and bacterial biomass (sample from 31 cm bsf). The concentration of both archaeal and bacterial lipids decreased just above and below this sediment horizon. At the SMT, the ratio of *sn2*-hydroxyarchaeol relative to archaeol was 1.6:1 (Table 3). Other diagnostic archaeal isoprenoidal hydrocarbons such as 2,6,11,15-tetramethylhexadecane (crocetane) could not be quantified due to an unresolved complex mixture of hydrocarbons (UCM) in all of the hydrocarbon fractions. Similarly, specific archaeal diethers and bacterial FAs could not be resolved from this background below 40 cm sediment depth. The concentrations of diagnostic archaeal lipids were roughly one order of magnitude lower in comparison to specific bacterial FAs.

The FA fraction in sediments at the SMT was dominated by the FAs $C_{16:1\omega5}$ and $cyC_{17:0\omega5,6}$ which are putatively specific for SRB involved in AOM (Elvert et al., 2003) and contained comparably high amounts of the FA $C_{17:1\omega6}$

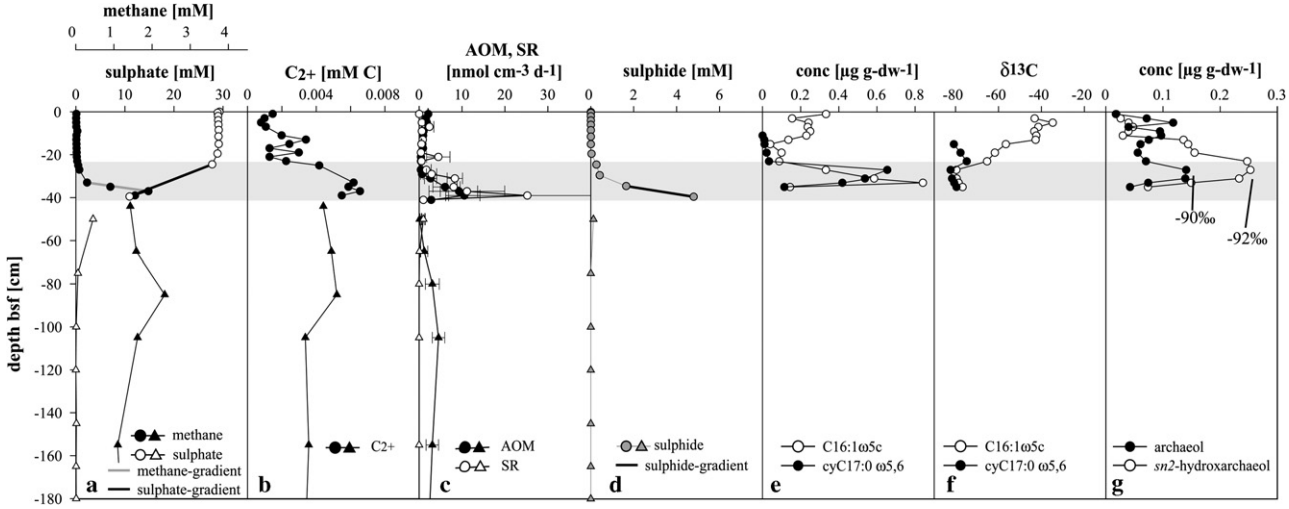

Fig. 4. Captain Arutyunov mud volcano. A distinct SMT, highlighted in grey, was found between 25 and 40 cm bsf (a). At this horizon, concentrations of higher hydrocarbons also decline (b). Note that AOM and SR rates (c), sulphide concentrations (d), concentrations (e) and stable carbon isotope values of diagnostic, bacterial fatty acids (f) and concentrations of isoprenoidal diethers (g) all peak at the SMT. (a) and (d) illustrate steepest gradients determined for methane, sulphate and sulphide (bold lines). Circles represent multiple-corer and triangles gravity corer samples. Errors are given as standard errors.

Table 3
Bacterial fatty acids, archaeal diether and isoprenoidal hydrocarbons analysed in sediments at the SMT of Captain Arutyunov and Bonjardim MV as well as in carbonate crusts from Hesperides and Faro MV

			Sediment		Carbonate	
			Captain Arutyunov	Bonjardim	Hesperides	Faro
Normalised abundance (δ^{13}C-values)	Bacterial fatty acids	$C_{14:0}$	1.3 (-75)	2.0 (-37)	1.1 (-31)	2.3 (-93)
		i-$C_{15:0}$	1.0 (-71)	1.0 (-42)	1.0 (-39)	1.0 (-99)
		ai-$C_{15:0}$	1.3 (-73)	8.4 (-47)	1.5 (-43)	1.9 (-95)
		$C_{15:0}$	0.6 (-73)	1.4 (nd)	0.3 (-45)	0.4 (-96)
		i-$C_{16:0}$	0.2 (-73)	nd	0.2 (nd)	0.2 (-87)
		$C_{16:1\omega9}$	0.7 (-65)	nd	nd	0.1 (-92)
		$C_{16:1\omega7}$	0.8 (-67)	14.6 (-34)	0.6 (-27)	1.8 (-93)
		$C_{16:1\omega5}$	7.7 (-80)	8.4 (-49)	0.1 (-41)	0.7 (-96)
		$C_{16:0}$	2.4 (-67)	7.8 (-21)	4.8 (-27)	1.6 (-77)
		10 Me$C_{16:0}$	0.3 (-67)	nd	nd	1.0 (-94)
		i-$C_{17:0}$	0.3 (-69)	nd	0.3 (-32)	0.3 (-96)
		ai-$C_{17:0}$	0.1 (nd)	1.1	0.5 (-38)	0.3 (-99)
		$C_{17:1\omega7}$	0.9 (-68)	1.9	0.5 (-31)	0.4 (-93)
		$C_{17:1\omega6}$	1.9 (-74)	nd	nd	0.1 (nd)
		cy$C_{17:0\omega5,6}$	7.1 (-82)	nd	nd	nd
		$C_{17:0}$	nd	nd	0.2 (nd)	0.1 (nd)
		$C_{18:1\omega9}$	1.0 (-27)	6.4 (-27)	0.2 (nd)	0.3 (-77)
		$C_{18:1\omega7}$	0.9 (-31)	13.7 (-31)	0.4 (-37)	1.5 (-84)
		$C_{18:0}$	0.2 (-25)	3.5 (-25)	1.8 (-28)	0.4 (-67)
	Archaeal lipids	Archaeol	1.0 (-90)	1.0 (-81)	1.0 (-97)	1.0 (-114)
		sn2-hydroxyarchaeol	1.7 (-92)	0.7 (-83)	tr	0.2 (-111)
		Crocetane / Phytane			0.5 (-47)	3.3 (-110)
		PMI:0			1.0 (-87)	1.0 (-111)
		ΣPMI:1			0.3 (nd)	4.6 (-113)
		ΣPMI:2			nd	8.3 (-113)
		ΣPMI:3			nd	0.3 (-101)
Concentration [µg g-dw^{-1}]	Bacterial fatty acids	i-$C_{15:0}$	0.08	0.01	0.1	8.7
		ai-$C_{15:0}$	0.1	0.09	0.15	16.77
		$C_{16:1\omega5}$	0.6	0.09	0.01	6.05
		$C_{17:1\omega6}$	0.14	nd	nd	0.5
		cy$C_{17:0\omega5,6}$	0.56	nd	nd	nd
	Archaeal lipids	Archaeol	0.14	0.4	2.39	41.58
		sn2-hydroxyarchaeol	0.23	0.3	0.02	8.31
		Crocetane / Phytane			0.23	4.59
		PMI:0			0.44	1.4
Putative origin			ANME2 Seep-SRB1	ANME1 Seep-SRB1 & ANME2 Seep-SRB1	ANME1 Seep-SRB1 (?)	ANME1 Seep-SRB1 & ANME2 Seep-SRB1

Abundances of fatty acids were normalised to i-$C_{15:0}$, archaeal diethers to archaeol and archaeal isoprenoidal hydrocarbons to PMI:0. Specific lipid components are highlighted in grey.

(Table 3). Both, $C_{16:1\omega5}$ and cy$C_{17:0\omega5,6}$ were the most ^{13}C-depleted FAs. However, all other FAs in the C_{14}–C_{17} range carried significantly ^{13}C-depleted isotope signatures as well with values ranging between −65‰ ($C_{16:1\omega9}$) and −75‰ ($C_{14:0}$). C_{18}-FAs were comparably enriched in ^{13}C with δ^{13}C-values ranging between −25‰ ($C_{18:0}$) and −31‰ ($C_{18:1\omega7}$) most likely indicating a planktonic origin of these compounds. Concentrations of mono- and dialkyl glycerol ethers (MAGEs and DAGEs, respectively), presumably of bacterial origin (Pancost et al., 2001), were low in all samples recovered during cruise SO-175. Thus, a detailed analysis of these compounds was not carried out. However, sediments at the SMT of Capt. Arutyunov MV comprised comparably high contents of MAGEs relative to DAGES with δ^{13}C-values ranging from −65‰ to −85‰ (data not shown). The MAGEs comprised a suite of alkyl moieties, which is comparable to those of the fatty acids found at Capt. Arutyunov MV. The suite of fatty acids extracted from the tubeworms comprised dominant amounts of the FAs $C_{16:1\omega7}$ and $C_{18:1\omega7}$ and to a lesser degree $C_{16:0}$ and $C_{18:0}$ with uniform δ^{13}C-values of about −40‰, indicating chemoautotrophic carbon fixation (data not shown). The alcohol and hydrocarbon fractions were not analysed.

3.2.4. Phylogenetic diversity

An archaeal and a bacterial clone library was constructed to study the 16S rDNA-based microbial diversity in sediments at the SMT of Capt. Arutyunov MV (30–40 cm bsf). The 16S rDNA archaeal clone library consisted of nine phylogenetic groups (Table 4). Closest relatives of these groups were found among seep-endemic, uncultured microorganisms. The majority of sequences obtained were related to the ANME-2 group (59% ANME-2a, 3% ANME-2c of all archaeal sequences) which is known to mediate AOM (Boetius et al., 2000; Orphan et al., 2002; Knittel et al., 2005). The second most abundant group (18% of all archaeal sequences) was found to belong to the ANME-1 cluster which is also known to mediate AOM (Hinrichs et al., 1999; Michaelis et al., 2002; Orphan et al., 2002). The bacterial clone library consisted of 10 uncultivated bacterial lineages. Similar to the archaeal sequences, the next relatives of all bacterial 16S rDNA sequences belonged to uncultivated organisms that are commonly found at methane seeps (Knittel et al., 2003; Table 4). The closest relatives of the most abundant cluster of sequences (81%) belonged to the Seep-SRB1 group which comprises the bacterial partners of ANME-1 and ANME-2 (Knittel et al., 2003). Other phylogenetic groups of *Bacteria* were represented by single sequences (<2%).

3.3. Bonjardim MV

3.3.1. Methane, C_{2+}, sulphate and sulphide

A distinct SMT was observed in the top metre of the gravity core section with *ex situ* methane concentrations above saturation at atmospheric pressure and sulphate concentrations dropping below 0.2 mM. After aligning the sulphate profile of the gravity core with the MUC-core section, the actual depth of the SMT was determined between 45 and 70 cm bsf (Fig. 5a). Methane concentrations in surface sediments (0–52 cm sediment depth) were <0.001 mM indicating a complete consumption of methane in the SMT. As the two core sections overlapped, concentration gradients were determined from the gravity core section and also from aligned profiles in the overlapping zone (Fig. 5a, d). The steepest methane and sulphate gradients in the gravity core section were determined with 0.09 and −0.76 µmol cm^{-4}, respectively (Fig. 5a, Table 2). Aligning the gravity core and MUC-core sections, the steepest sulphate gradient was −1.67 µmol cm^{-4}. Methane concentrations declined

Table 4
Archaeal and bacterial 16S rDNA clone libraries obtained from sediments of the SMT of Captain Arutyunov MV

Phylogenetic group		Clones	Representative clone	Next relative	Sequence similarity (%)
Archaea		39			
Euryarchaeota	ANME-2a	23	CAMV300A948 (DQ004662)	Uncultured cold seep archaeal clone BS-K-H6 (AJ578128)	99
	ANME-2c	1	CAMV301A975 (DQ004668)	Uncultured hydrocarbon seep archaeal clone C1_R019 (AF419638)	99
	ANME-1	7	CAMV300A952 (DQ004664)	Uncultured hydrocarbon seep archaeal clone HydCal61 (AJ578089)	99
	Marine benthic group D	1	CAMV300A963 (DQ004667)	Uncultured hydrothermal vent archaeal clone pMC2A203 (AB019737)	98
	Marine benthic group D	1	CAMV300A951 (DQ004663)	Uncultured contaminated aquifer archaeal clone WCHD3-02 (AF050616)	90
	Marine benthic group D	1	CAMV301A980 (DQ004669)	Uncultured hydrothermal vent archaeal clone VC2.1 Arc6 (AF068817)	87
	Unclassified archaea	1	CAMV300A960 (DQ004666)	Uncultured cold seep archaeal clone BS-SR-H5 (AJ578148)	98
	Unclassified archaea	3	CAMV301A993 (DQ004661)	Uncultured hydrothermal vent archaea clone NT07-CAT-A24 (AB111475)	80
Crenarchaeota	Marine benthic group B	1	CAMV300A958 (DQ004665)	Uncultured archaeal clone BS-K-D4 (AJ578124)	99
Bacteria		47			
δ Proteobacteria	Seep-SRB1	38	CAMV300B922 (DQ004675)	Uncultured hydrocarbon seep bacterial clone Hyd89-04 (AJ535240)	99
	Desulfobulbacteraceae	1	CAMV301B937 (DQ004679)	Uncultured Echinocardium cordatum hindgut bacterial clone Del 7 (AY845643)	96
	Desulfobulbaceae	1	CAMV300B921 (DQ004674)	Uncultured hydrocarbon seep bacterial clone Hyd89-51 (AJ535252)	99
γ Proteobacteria	Stenotrophomonas	1	CAMV301B944 (DQ004671)	Stenotrophomonas maltophilia (AB008509)	99
Clostridia	Clostridiales	1	CAMV300B902 (DQ004670)	Uncultured bacterial clone DR9IPCB16SCT8 (AY604055)	98
Spirochaetes	Spirochaeta	1	CAMV301B941 (DQ004680)	Uncultured Spirochaeta sp. (AF424377)	96
	Spirochaeta	1	CAMV300B915 (DQ004672)	Uncultured spirochete clone IE052 (AY605138)	96
	Unclassified bacteria	1	CAMV300B916 (DQ004673)	Uncultured hydrocarbon seep bacterial clone Hyd24-12 (AJ535232)	97
	Unclassified bacteria	1	CAMV301B934 (DQ004678)	Uncultured hydrocarbon seep bacterial clone 1B-41 (AY592596)	93
	Unclassified bacteria	1	CAMV300B923 (DQ004676)	Uncultured hydrocarbon seep bacterial clone GCA025 (AF154106)	98

The Archaeal clone library is dominated by sequences belonging to the ANME-2 cluster and the bacterial library by sequences belonging to the Seep-SRB1 cluster.

below the depth at which the two core sections overlap (Fig. 5a). Hence, no further concentration gradient was determined. In comparison to Capt. Arutyunov MV, C_{2+}-concentrations were high with values of >0.25 mM at a sediment depth below 1 m (Fig. 5b). Similar to methane, concentrations of C_{2+}-compounds decreased across the SMT indicating a consumption of these compounds. Gaseous hydrocarbons comprised methane (>81%), ethane (<14%), propane (<4.5%) and Σbutane (<0.4%) indicating a thermogenic origin of these gases (Stadnitskaia et al., 2006). Sulphide concentrations peaked in the SMT with 5.3 mM at 52.5 cm bsf (Fig. 5d). In the gravity core section, the steepest sulphide gradients were determined as 0.23 (upward) and −0.07 (downward) μmol cm^{-4}, respectively (Table 2). Aligning the two core sections, the steepest (upward) sulphide gradient was determined with 0.73 μmol cm^{-4}.

3.3.2. AOM, SR rates and diffusive fluxes

AOM and SR rates were highest in the SMT at 58 cm bsf with maximum values of 2.6 and 15.4 nmol cm^{-3} d^{-1}, respectively (Fig. 5c). Comparably low values of AOM and SR rates were measured in over- and underlying sediment horizons. Replicate AOM and SR rate measurements showed a high standard error of 92% and 85% of the average value, respectively, possibly indicating a high small

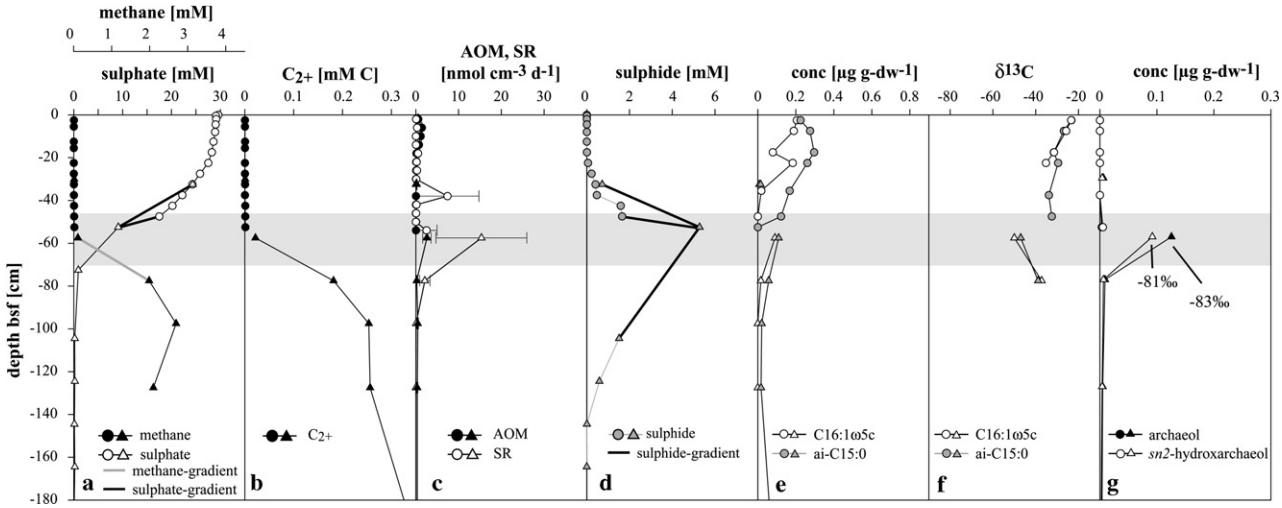

Fig. 5. Bonjardim mud volcano. A distinct SMT, highlighted in grey, was found between 50 and 70 cm bsf (a). At this horizon, concentrations of higher hydrocarbons also decline (b). Note that concentrations of C_{2+}-compounds are ~35-fold higher compared to Captain Arutyunov MV. AOM and SR rates (c), sulphide concentrations (d), concentrations (e) and stable carbon isotope values of diagnostic, bacterial fatty acids (f) and concentrations of isoprenoidal diethers (g) peak at the SMT. (a) and (d) illustrate steepest gradients determined for methane, sulphate and sulphide (bold lines). Concentration gradients for sulphate and sulphide were determined from concentration profiles of the gravity core samples as well as from aligned gravity core and multiple-corer concentration profiles. Circles represent multiple-corer and triangles gravity corer samples. Errors are given as standard errors.

scale variability on a metre scale. The 19-fold higher areal SR compared to AOM suggests a decoupling of these two processes (Table 2). Accordingly, the concentration gradients (determined from unaligned and aligned profiles) translate to a 5.1–11-fold higher diffusive downward flux of sulphate compared to the upward flux of methane. The cumulative sulphide flux (upward and downward) accounted for 77–92% of the sulphate flux.

3.3.3. Lipid biomarker

A moderate increase of diagnostic archaeal and bacterial lipid concentrations was observed at the SMT in sediments of Bonjardim MV (Fig. 5e, g). At this horizon (−57 cm bsf), stable carbon isotope analysis revealed highest depletions in ^{13}C with minimum values of −83‰ (*sn2*-hydroxyarchaeol) in archaeal diether lipids and −49‰ ($C_{16:1\omega5}$) in bacterial FAs (Table 3, Fig. 5f, g). At the SMT, the ratio of *sn2*-hydroxyarchaeol relative to archaeol was 0.7:1 and therefore lower in comparison to Capt. Arutyunov MV (Table 3). Similar to Capt. Arutyunov MV, other diagnostic archaeal isoprenoidal hydrocarbons could not be measured due to a high UCM background. Equally high amounts of the FAs $C_{16:1\omega5}$ and ai-$C_{15:0}$, both of which were the most ^{13}C-depleted FAs (Table 3), were detected in sediments at the SMT. The FA cy$C_{17:0\omega5,6}$, which was abundant at Capt. Arutyunov MV could not be detected in sediments of Bonjardim MV. Furthermore, dominant FAs such as $C_{16:1\omega7}$, $C_{16:0}$, $C_{18:1\omega9}$ and $C_{18:1\omega7}$ carried $\delta^{13}C$-signatures $\geqslant -34‰$, indicating that AOM was not the main energy and carbon delivering process to the microbial community. In contrast to Capt. Arutyunov MV, the concentrations of diagnostic archaeal lipids were roughly 4-fold higher compared to specific bacterial FAs (Table 3). A further analysis of the diversity of microbial organism using 16S rDNA methods was not carried out at Bonjardim MV.

3.4. Ginsburg MV, Gemini MV and "No Name"

3.4.1. Methane, sulphate and sulphide

The SMT was located in the upper metre of the sediment cores retrieved from Ginsburg and Gemini MV and at 2–3 m bsf at the "No Name" structure, respectively (Fig. 6a, c, e). Methane concentrations in sediments overlying the SMT at these structures were <0.001 mM, and reached *ex situ* concentrations above (Gemini MV and "No Name") and just below saturation (1.3 mM, Ginsburg MV) below the SMT. Sediments retrieved from Ginsburg MV had a distinct smell of petroleum below 40 cm bsf. No depth corrections were made as only gravity cores were taken from these MVs. The actual depth of the SMTs was therefore most likely 10–40 cm below the sediment depth indicated in Fig. 6. In contrast to the observed depletion of sulphate to concentrations <0.4 mM below the SMT at Gemini MV and the "No Name" structure, sulphate concentrations showed a minimum between 30 and 70 cm and an increase to values $\geqslant$17 mM with depth below 90 cm at Ginsburg MV. The total diffusive sulphate flux was therefore calculated from both, the upward and the downward gradients at Ginsburg MV. At Ginsburg MV, Gemini MV and the "No Name" structure, methane and downward sulphate gradients ranged from 0.02 to 0.05 and −0.11 to −0.92 µmol cm^{-4}, respectively (Table 2). The upward sulphate gradient at Ginsburg MV was 0.35 µmol cm^{-4}. Sulphide concentrations peaked in the SMTs with values between 4.7 and 7.6 mM (Fig. 6b, d, f)

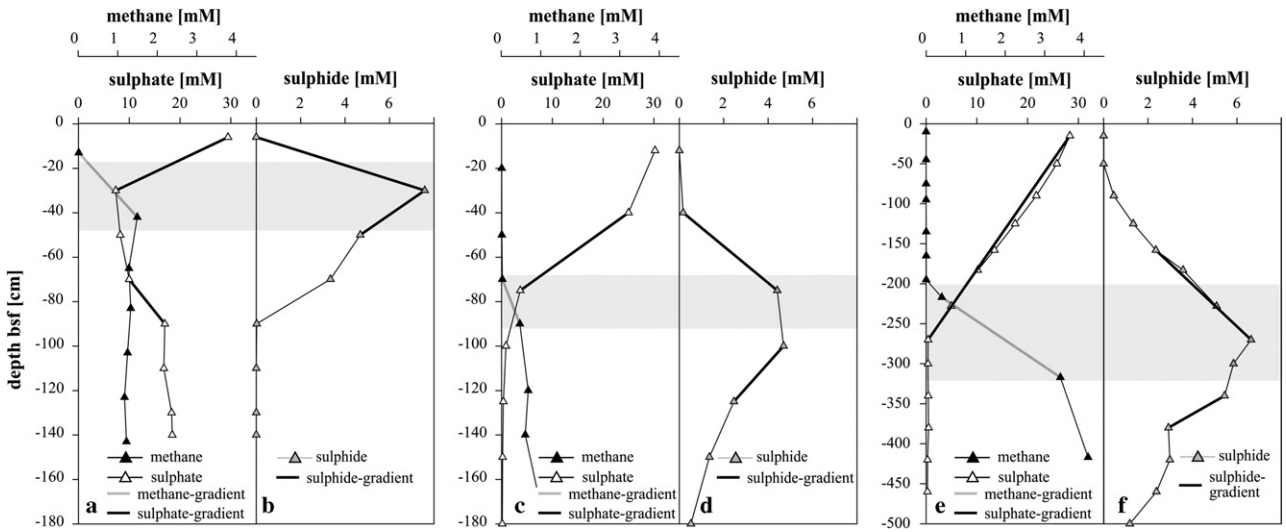

Fig. 6. The SMT, highlighted in grey, was found in the top most m at Ginsburg (a) and Gemini (c) and between 2 and 3 m at No Name MV (e; note the different scale chosen for depth). In these horizons, also sulphide concentrations peak (b, d, f). Bold lines illustrate steepest gradients determined for methane, sulphate and sulphide.

and steepest gradients were determined with values between 0.04 to 0.32 (upward) and −0.06 to −0.15 (downward) μmol cm^{-4}, respectively (Table 2).

3.4.2. Diffusive fluxes

The diffusive flux calculations from pore water profiles of Ginsburg MV, Gemini MV and the "No Name" structure indicate that the diffusive sulphate fluxes exceeded the methane fluxes (by 15.5-, 18.5- and 2.5-fold, respectively, according to the calculation). This suggests a decoupling of AOM and SR at these structures similar to the observations made at Bonjardim MV (Table 2). The calculated cumulative (upward + downward) sulphide flux accounted for 66%, 70% and 146% of the sulphate fluxes at Ginsburg MV, Gemini MV and the "No Name" structure, respectively. The composition of the microbial community was not investigated here.

3.5. Lipid biomarkers of carbonate crusts

Exposed carbonate crusts were observed at the mud volcanoes Ginsburg, Hesperides and Faro. Additionally, high amounts of broken carbonate chimneys were found at Hesperides and Faro MV. Both crusts and chimney pieces were absent at Capt. Arutyunov MV, Bonjardim MV and the "No Name" structure according to our visual inspections. We could retrieve crust samples from the summits of Hesperides and Faro MV for further analyses of the lipid signatures of the crusts.

3.5.1. Hesperides MV

Carbonate crusts of Hesperides MV contained archaeal and bacterial lipids diagnostic for methanotrophic communities and processes. Archaeal lipids were strongly depleted in $\delta^{13}C$ with minimum values of −97‰ (archaeol) whereas bacterial FAs were only moderately depleted with minimum values of −43‰ (ai-$C_{15:0}$, Table 3). Only trace amounts of *sn2*-hydroxyarchaeol were detected among the archaeal diethers. Isoprenoidal hydrocarbons were dominated by 2,6,10,15,19-pentamethylicosane (PMI:0) and contained comparably low amounts of a crocetane/2,6,10,14-tetramethylhexadecane (phytane) mixture and ΣPMI:1 (comprising 2 isomers). The FA fraction in the carbonate was dominated by $C_{16:0}$ followed by $C_{18:0}$ with $\delta^{13}C$-values >−28‰ (Table 3). FAs putatively specific for SRB involved in AOM such as $C_{16:1\omega5}$, i-$C_{15:0}$ and ai-$C_{15:0}$ (Elvert et al., 2003; Blumenberg et al., 2004), were approximately 3–4.8 times lower in concentration compared to $C_{16:0}$. However, in contrast to abundant FAs, stable carbon isotope compositions of i-$C_{15:0}$, ai-$C_{15:0}$ and $C_{16:1\omega5}$ showed a moderate depletion in ^{13}C (Table 3). Moreover, in comparison to specific archaeal lipids, diagnostic bacterial FAs were roughly an order of magnitude lower in concentration.

3.5.2. Faro MV

All archaeal and bacterial lipids found in the carbonate crust of Faro MV were strongly depleted in ^{13}C (Table 3) with minimum $\delta^{13}C$-values of −114‰ (archaeol) in diagnostic archaeal diether lipids and −99‰ (i-$C_{15:0}$) in specific bacterial FAs (Table 3). Archaeal diether lipids were dominated by archaeol and contained comparably low amounts of *sn2*-hydroxyarchaeol. Isoprenoidal hydrocarbons were dominated by PMI:2 (9 isomers) followed by PMI:1 (2 isomers) and relatively high amounts of crocetane/phytane. Specific FAs showed comparably small differences in abundance and $\delta^{13}C$-values (Table 3). However, ai-$C_{15:0}$ was the most dominant FA with a roughly 2-fold higher concentration compared to i-$C_{15:0}$ and $C_{16:1\omega5}$. The FA cy$C_{17:0\omega5,6}$ was not detected. Concentrations of specific FAs were comparable to specific archaeal lipids.

4. Discussion

4.1. Evidence of methane-driven geochemical and biological activity at mud volcanoes of the Gulf of Cadiz

Active marine mud volcanoes have been identified as important escape pathways of hydrocarbon gases and may even contribute to atmospheric green house gases (Dimitrov, 2002; Judd et al., 2002; Kopf, 2002; Damm and Budéus, 2003; Dimitrov, 2003; Sauter et al., 2006). However, high methane fluxes reaching surface sediments may support high biomasses of methane-oxidizing microorganisms, and via their sulphide production also thiotrophic, giant bacteria and other chemosynthetic fauna which form a filter against gas emission to the hydrosphere (Olu et al., 1997b; Sahling et al., 2002; Werne et al., 2002; Boetius and Suess, 2004; Milkov et al., 2004; Cordes et al., 2005). Furthermore, methane venting is often associated with the precipitation of authigenic carbonates which sequester methane derived CO_2 at the seafloor (Aloisi et al., 2000; Kopf, 2002; Boetius and Suess, 2004; Hensen et al., 2004). These carbonates may also serve as paleo-indicators of previously active phases of quiescent or fossil seeps (Ritger et al., 1987; Peckmann et al., 1999; Thiel et al., 1999).

The Gulf of Cadiz is characterised by numerous mud volcanoes (Fig. 1) which have been intensely surveyed since their discovery in 1999 (Kenyon et al., 2000, 2001; Somoza et al., 2002; Pinheiro et al., 2003). Among the findings indicative of high past and present methane seepage are the occurrence of hydrate-bearing sediments, authigenic carbonates and seep related biota at several mud volcanoes (Gardner, 2001; Diaz-Del-Rio et al., 2003; Pinheiro et al., 2003; Somoza et al., 2003). Yet, the present activity of these structures in relation to methane emission to the hydrosphere remains unknown. The observations during cruise SO-175 revealed only few traces of methane reaching surface sediment horizons (here referring to the upper decimetres bsf reachable by biota) at the centres of the mud volcanoes Capt. Arutyunov, Bonjardim, Ginsburg and Hesperides, and the "No Name" structure. No visible fluid or gas escape to the hydrosphere was detected with video observations, indicating that the mud volcanoes may be relatively inactive and that the methane flux may be consumed within subsurface sediment horizons. In contrast, highly active seep systems such as Hydrate Ridge, the Gulf of Mexico or Håkon Mosby Mud Volcano show maximal methane consumption and sulphide production at the sediment surface, and emit methane into the hydrosphere through focused gas and fluid escape pathways, despite the high methane and sulphate turnover rates consuming substantial fractions of the methane flux (Boetius et al., 2000; Damm and Budéus, 2003; Treude et al., 2003; Joye et al., 2004; De Beer et al., 2006; Sauter et al., 2006).

The high sulphide fluxes from anaerobic methane consumption at active seeps are utilised by thiotrophic communities, e.g. mats of giant bacteria like *Beggiatoa* sp., various chemosynthetic bivalves like *Calyptogena* sp., *Acharax* sp., *Bathymodiolus* sp. and by several siboglinid tubeworm species (Sibuet and Olu, 1998). Such communities often colonise large areas at highly active seeps. Furthermore, these organisms are adapted to different geochemical settings and can be used as indicators for high methane fluxes and turnover in surface sediments. Three types of indicator communities were so far observed at low abundances at the investigated mud volcanoes. Some small (ca. 20 cm diametre) blackish sediment patches covered with white bacterial mats were observed by towed camera systems at Faro MV indicating locally elevated fluxes of sulphide (likely AOM-derived) reaching the surface of the seafloor (Fig. 6d). Few specimen of the deep-dwelling thiotrophic bivalve *Acharax* sp. were recovered from Faro MV and previously from Ginsburg MV (Gardner, 2001). Members of the family *Solemyidae* to which *Acharax* sp. belongs are mostly deep burrowing and occur in seep habitats with low or moderate methane and sulphide fluxes where they can take up sulphide through their foot from subsurface accumulations (Sibuet and Olu, 1998; Sahling et al., 2002; Treude et al., 2003). At Hydrate Ridge for instance, *Acharax* sp. mines subsurface sediments for sulphide pockets below 15 cm sediment depth (Sahling et al., 2002). As a third indicator species, tubeworms were recovered from Capt. Arutyunov and previously observed at Bonjardim MV (Pinheiro et al., 2003). As adult animals, these worms are lacking a mouth, gut and anus and are hence depending on energy and carbon sources provided by symbiotic, thiotrophic or methanotrophic bacteria (Southward et al., 1981; Dando et al., 1994; Gebruk et al., 2003; Southward et al., 2005). At Capt. Arutyunov MV, the moderate ^{13}C-depletion of worm-derived membrane lipids (ca. $-40‰$) indicates a thiotrophic or mixed methanotrophic/thiotrophic feeding mode of the tubeworm symbionts. This is concluded on the basis of the $\delta^{13}C$-value of $-48‰$ of the source methane (Nuzzo et al., 2005). Aerobic methanotrophic bacteria are characterised by a considerable depletion in the ^{13}C-content of membrane lipids in comparison to source methane (Hanson and Hanson, 1996), which was not reflected in the tubeworm isotope signature.

4.2. Hotspots of hydrocarbon turnover at the mud volcanoes of the Gulf of Cadiz

The observed patterns of seep related biota is in good agreement with the observed geochemical gradients. All mud volcanoes investigated here showed a complete depletion of methane and sulphate within the subsurface SMT. At Capt. Arutyunov and Bonjardim MV, the SMT was positioned at 25–40 cm and 45–70 cm bsf, respectively (Figs. 4, 5a), and reflected in elevated AOM and SR rates within this zone. Generally, integrated rate measurements were comparable to the diffusive fluxes at Capt. Arutyunov and Bonjardim MV (Table 3). Also, concentration measurements of methane and sulphate and the resulting estimates of diffusive methane and sulphate fluxes at Ginsburg MV, Gemini MV and the

"No Name" structure indicate that sulphate-dependent AOM is a widespread microbial process in the centres of the mud volcanoes of the Gulf of Cadiz. However, as we cannot exclude a potential advective transport component in sediments of the surveyed mud volcanoes and due to shortcomings in the vertical resolution of pore water profiles, the estimates of fluxes presented here should be considered with caution.

With respect to methane fluxes and microbial turnover rates at the time of our investigation, Capt. Arutyunov MV was the most active of the investigated structures followed by Bonjardim, Ginsburg and Gemini MV, while "No Name" was the least active structure (Table 2). Furthermore, highest turnover rates and fluxes coincided with the shallowest SMT comparing all investigated MVs. Hence, compared to other marine gas seeps and methane-rich environments, the Gulf of Cadiz MVs investigated here showed a low or medium range in methane turnover rates, reflecting the relatively low methane fluxes. At the Namibian continental slope, the north western Black Sea and Chilean shelf and the western Argentinean basin for instance, the SMT is located several metres bsf and methane fluxes are low with values usually <55 mmol m^{-2} $year^{-1}$ (Niewöhner et al., 1998; Jørgensen et al., 2001; Hensen et al., 2003; Treude et al., 2005). These values are comparable to Ginsburg and Gemini MV as well as to the "No Name" structure. The AOM activity and diffusive methane fluxes at Capt. Arutyunov and Bonjardim MV were substantially higher than those at Ginsburg MV, Gemini MV and the "No Name" structure. However, areal rates and diffusive fluxes at Capt. Arutyunov and Bonjardim MV are still two orders of magnitude lower in comparison to other cold seeps, which bear gas hydrates at their stability limit such as Håkon Mosby Mud Volcano, Hydrate Ridge and the Gulf of Mexico. In such environments with active fluid flow (>100 cm $year^{-1}$) and gas emission via ebullition, methane fluxes were estimated with values >8.5 mol m^{-2} $year^{-1}$ (Torres et al., 2002; Luff and Wallmann, 2003; De Beer et al., 2006) and AOM reached values >4 mol m^{-2} $year^{-1}$, i.e. >0.5 μmol cm^{-3} d^{-1} (Treude et al., 2003; Joye et al., 2004).

In vitro experiments with sediment slurries and *ex situ* tracer injection assays have previously shown that AOM and SR are in a 1:1 molar stoichiometry if methane is the sole carbon source (Nauhaus et al., 2002; Treude et al., 2003). In spite of the putative loss of methane during subsampling, the deviation from the 1:1 stoichiometry between AOM and SR as well as between the sulphate and methane fluxes (Table 2) indicates the presence of electron donors other than methane for SR at the investigated MVs. SRR were always highest at the depth of the SMT but just above detection limit in the overlying sediments of Capt. Arutyunov and Bonjardim MV (Figs. 4, 5c). Hence, a substantial contribution to SR by pelagic organic matter input can be ruled out. However, our data provide evidence for the presence of other hydrocarbons beside methane in the subsurface sediments of several mud volcanoes. Sulphate reducing bacteria can use a variety of short and long chain alkanes and complex aliphatic and aromatic compounds (Rueter et al., 1994; Widdel and Rabus, 2001). At Capt. Arutyunov and Bonjardim MV the presence of complex hydrocarbons is indicated by the strong unresolved complex mixture (UCM) of hydrocarbons in sediment samples from the SMT and deeper sediment horizons. Furthermore, C_2–C_4 compounds declined at the depth of the SMT (Figs. 4, 5b), indicating their consumption in this zone. At Bonjardim MV, the deviation between AOM and SR was higher compared to Capt. Arutyunov MV coinciding with higher concentrations of C_{2+} compounds. Furthermore, Mazurenko et al. (2002) observed a composition of hydrocarbon gases at Ginsburg MV similar to those detected at Bonjardim MV. Nuzzo et al. (2005) and Stadnitskaia et al. (2006) showed that methane is commonly of a thermogenic origin at mud volcanoes in the Gulf of Cadiz. Hence, SR fuelled by higher hydrocarbons could be an important microbial process in the MV sediments of the Gulf of Cadiz in addition to methane oxidation. Similar results were obtained in a study of cold seeps of the Gulf of Mexico where SR rates exceed AOM rates up to 10-fold, fuelled by a variety of hydrocarbons and petroleum in the sediments (Joye et al., 2004).

In conclusion, our biogeochemical measurements as well as biological and geological observations indicate that elevated methane fluxes are associated with the centres of the MVs studied during cruise SO-175. However, at the investigated sites, all methane was consumed anaerobically in subsurface sediments and we could not observe any emission of methane to the hydrosphere. However, there is evidence for extensive fluid and/or gas escape in the past as indicated by the widespread occurrence of massive carbonate chimneys and crusts (Diaz-Del-Rio et al., 2003; Somoza et al., 2003) of which at least the latter bear AOM signals. Another geological evidence for temporally varying activities of mud volcanism in the Gulf of Cadiz are the typical "Christmas tree" structures observed on high-resolution seismic profiles (Somoza et al., 2002, 2003). Such patterns are probably caused by eruptive events followed by phases of dormancy. This so-called multiphase activity is a common behaviour in many terrestrial mud volcanoes (e.g. Lokbatan MV; Aliyev et al., 2002; Kholodov, 2002; Dimitrov, 2003). It is therefore possible that mud volcanism in the Gulf of Cadiz is in a transient state of low activity at present.

4.3. Identity of methane oxidising communities in sediments and carbonate crusts

Fingerprinting of diagnostic lipids is a common tool for the chemotaxonomic identification of microorganisms (Madigan et al., 2000; Boschker and Middelburg, 2002). This approach has been used extensively to examine anaerobic methanotrophic organisms, because the carbon isotope fractionation associated with AOM leads to specific, very depleted $\delta^{13}C$-signatures of lipid biomarkers (Hinrichs

et al., 1999; Elvert et al., 2001; Blumenberg et al., 2004). The dominance of bacterial and archaeal lipids with low δ^{13}C-values in sediments and carbonates indicate that AOM is a major biomass-generating process at the investigated MVs. Differences in the abundances of specific archaeal isoprenoidal diethers, hydrocarbons and bacterial FAs, as well as varying $\Delta\delta^{13}$C-values of these lipids (compared to source methane) indicate that several phylogenetic groups of methanotrophic communities mediate AOM in the Gulf of Cadiz. Elevated concentrations and associated low δ^{13}C-signatures of specific archaeal and bacterial membrane lipids corresponded with elevated AOM and SR rates in sediments of the SMT at Capt. Arutyunov and Bonjardim MV (Figs. 4, 5e–g, Table 3). In combination with 16S rDNA analysis, the biomarker patterns give evidence that AOM is mediated by a microbial community consisting of methanotrophic archaea and SRB phylogenetically related to those which were previously found at other methane seeps (Boetius et al., 2000; Michaelis et al., 2002; Orphan et al., 2002; Teske et al., 2002; Niemann et al., 2005). Furthermore, the presence of a similar suite of ^{13}C-depleted lipids in abundant authigenic carbonates recovered from Hesperides and Faro MV (Table 3) indicates higher activities and a more widespread microbial methane turnover in the past.

4.3.1. Methanotrophic archaea

Previous publications revealed dominant amounts of *sn2*-hydroxarchaeol relative to archaeol in ANME-2 dominated habitats, whereas the reverse was observed in ANME-1 dominated systems (Blumenberg et al., 2004; Elvert et al., 2005; Niemann et al., 2005). Moreover, ANME-2 communities were found to comprise high contents of crocetane, whereas it seems to be present at low concentrations in ANME-1 (Elvert et al., 1999; Boetius et al., 2000; Blumenberg et al., 2004). Stable carbon isotope fractionations were found to be higher in ANME-2 compared to ANME-1 dominated habitats (Orphan et al., 2002) with $\Delta\delta^{13}$C-values (archaeol relative to the source methane) ranging between 34 to 53‰ and 11 to 37‰, respectively (Hinrichs et al., 1999; Boetius et al., 2000; Elvert et al., 2001; Orphan et al., 2002; Teske et al., 2002; Blumenberg et al., 2004; Niemann et al., 2005).

In the Gulf of Cadiz, a high *sn2*-hydroxyarchaeol to archaeol ratio of 1.7:1 was detected at Capt. Arutyunov MV indicating that this system is dominated by ANME-2 archaea (Blumenberg et al., 2004; Elvert et al., 2005). Accordingly, a high $\Delta\delta^{13}$C-value of 42‰ of archaeol compared to the source methane (−48‰, Nuzzo et al., 2005) was observed. Furthermore, the dominance of ANME-2 compared to ANME-1 sequences in the clone library from Capt. Arutyunov MV suggests a dominance of ANME-2 in this SMT. However, the SMT of Capt. Arutyunov MV also contained other typical seep associated 16S rDNA sequences, including crenarcheota of the Marine Benthic Group B, which are often found at methane seeps, but whose function remains unknown (Knittel et al., 2005). At Bonjardim MV, a lower *sn2*-hydroxyarchaeol to archaeol ratio of 0.7:1 combined with lower $\Delta\delta^{13}$C-values between the biomarkers (e.g. archaeol, 31.5‰) relative to the source methane (−49.5 to −51‰, Nuzzo et al., 2005; Stadnitskaia et al., 2006) lie between published values from systems dominated by either ANME-1 or ANME-2 (Blumenberg et al., 2004; Elvert et al., 2005; Niemann et al., 2005). This suggests a mixed ANME community in these sediments. Similar characteristics have been observed in carbonate crusts at Faro MV. At this mud volcano, substantial amounts of ^{13}C-depleted crocetane were detected giving additional indications for an involvement of ANME-2 in AOM at the time of carbonate precipitation. At Hesperides MV, only trace amounts of *sn2*-hydroxyarchaeol were detected, and thus indicate the dominance of ANME-1 communities. No distinct environmental preferences have been found for either group, most likely because the taxonomic level investigated comprises a relatively large diversity of microorganisms.

4.3.2. Sulphate reducing bacteria

At many different cold seep settings, ANME-1 and ANME-2 archaea have been found in consortium with SRB of the Seep-SRB1 cluster belonging to the *Desulfosarcina/Desulfococcus* group (Knittel et al., 2003). However, this cluster apparently comprises physiologically different ecotypes that are distinguished by very specific FA patterns according to their association to either ANME-1 or to ANME-2 (Elvert et al., 2003; Blumenberg et al., 2004). FA signatures in environmental systems dominated by ANME-1/Seep-SRB1 communities comprise high contents of ai-$C_{15:0}$ relative to i-$C_{15:0}$ (Blumenberg et al., 2004; Elvert et al., 2005), whereas systems dominated by ANME-2/Seep-SRB1 communities comprise the unusual FA cy$C_{17:1\omega5,6}$ and dominant contents of $C_{16:1\omega5}$ but almost balanced ratios of ai-$C_{15:0}$ relative to i-$C_{15:0}$ (Elvert et al., 2003; Blumenberg et al., 2004).

The dominance of the unusual FAs $C_{16:1\omega5}$ and cy$C_{17:1\omega5,6}$ and an almost equal ratio of the iso- and ante-iso-branched $C_{15:0}$ FAs in sediments of the SMT at Capt. Arutyunov MV are in very good agreement with the archaeal lipid data and published lipid signatures of the Seep-SRB1 ecotype associated with ANME-2. This finding is also in accordance with the predominance of Seep-SRB1 sequences in the bacterial clone library. As expected from the detection of potentially diverse ANME communities at Bonjardim MV, the FA signature shows characteristics of both SRB ecotypes previously identified as bacterial partners in AOM. The high ratio of ai-$C_{15:0}$ compared to i-$C_{15:0}$ (8.4:1) is indicative for the Seep-SRB1 ecotype associated with ANME-1 while the high abundance of $C_{16:1\omega5}$ indicates the ecotype associated with ANME-2. This finding is similar to results obtained from a carbonate crust at Faro MV where a comparable fatty acid pattern has been detected. At Bonjardim MV, however, several FAs carry δ^{13}C-signatures that are comparable to the source methane and do not show any fractionation. This suggests

a contribution to carbon biomass from processes other than methane consumption. A similar mixture of carbon sources to biomass could also explain the unspecific signature of FAs in the carbonate of Hesperides MV.

Another striking difference is the comparably high lipid concentration in the carbonate recovered from Faro compared to that recovered from Hesperides MV. A rather recent formation of the sampled carbonate from Faro MV appears likely, as these were stained black from sulphide and recovered together with some living specimens of the chemosynthetic bivalve *Acharax* sp. A possible explanation for the difference in AOM-derived lipid contents could be that the sampled carbonate crust from Hesperides is older than that recovered from Faro MV and has been exposed to oxic sea water and lipid diagenesis for a longer time which is indicated by the dominant abundance of saturated FAs relative to unsaturated FAs. This may also explain the dominance of PMI's with higher degrees of saturation at Hesperides compared to Faro MV assuming that the diagenetic alteration of unsaturated isoprenoid hydrocarbons is similar to that of FAs.

5. Conclusions

At the centres of the mud volcanoes Captain Arutyunov, Bonjardim, Ginsburg, Gemini and Faro as well as at the "No Name" structure, several indications for a slow upward fluid and gas flux were found. Our data suggest a complete consumption of methane and higher hydrocarbons in the sediments of the studied mud volcanoes at depths of 20–300 cm below seafloor. We found no indication of hydrocarbons reaching near surface sediments or the hydrosphere except from the visual observation of small patches of reduced sediments covered by giant sulphide-oxidizing bacteria indicating localised near-surface AOM activities. However, with respect to the limited extend of video surveys and sediment sampling in this study, a potential seepage of hydrocarbons into the water column can not be ruled out. The overlap of methane and sulphate depletion with sulphide production shows that methane oxidation processes are mediated microbially under anaerobic conditions. Correspondingly, AOM and SR rates show a peak in a distinct, narrow SMT in the subsurface sediments of the mud volcano centres. Highest turnover rates and fluxes coincided with the shallowest SMT depths with Capt. Arutyunov MV as the most active system in the study area, followed by the mud volcanoes Bonjardim, Ginsburg and Gemini, and finally the "No Name" structure. In comparison to other gas seeps, methane fluxes and turnover rates are low to mid range in the Gulf of Cadiz. In addition to AOM, the anaerobic oxidation of higher hydrocarbons could be an important process fuelling SR. Lipid biomarker patterns and 16S rDNA clone sequences from the sediments and carbonates of the AOM hotspots provide evidence that both of the previously described ANME-1/Seep-SRB1 and ANME-2/Seep-SRB1 communities mediate AOM at mud volcanoes in the Gulf of Cadiz. The finding of their lipid signatures in carbonate crusts at the centres of the investigated mud volcanoes indicates that at least some of the vast amounts of carbonates littering mud volcanoes and diapiric ridges in the northern part of the Gulf of Cadiz are linked to methane seepage.

Acknowledgments

The authors thank the captain and crew as well as the shipboard scientific community of the R/V SONNE for their help at sea. We also thank Tomas Wilkop, Imke Müller and Viola Beier for technical assistance with laboratory analyses. Scientific exchange and collaboration were supported by the CRUP-ICCTI/DAAD Portuguese/German Joint Action *Geophere/Biosphere Coupling Processes in the Gulf of Cadiz* (A-15/04; Boetius, Pinheiro). This work was also supported by the ESF Eurocores/Euromargins MVSEIS project (01-LEC_EMA24F; PDCTM72003/DIV/40018-MVSEIS), as well as by the IRCCM (International Research Consortium on Continental Margins at International University Bremen, Germany), the Max Planck Society and the project MUMM (Mikrobielle Umsatzraten von Methan in gashydrathaltigen Sedimenten, FN 03G0608A) supported by the German Ministry of Education and Research (BMBF). This is publication GEOTECH-234 of the program GEOTECHNOLOGIEN of the BMBF and German Research Foundation (DFG).

Associate editor: Donald E. Canfield

References

Akhmanov, G., Woodside, J., 1998. Mud volcanic samples in the context of the mediterranean ridge mud diapiric belt. In: Robertson, A.H.F., Emeis, K.-C., Richter, C., Camerlenghi, A. (Eds.), Proceedings of the Ocean Drilling Program, Scienctific Results. Ocean Drilling Program, College Station, TX.

Aliyev, A.A., Guliyev, I.S., Belov, I.S., 2002. Catalogue of recorded eruption of mud volcanoes of Azerbaijan (for period of years 1810–2001). Nafta Press, Baker.

Aloisi, G., Bouloubassi, I., Heijs, S.K., Pancost, R.D., Pierre, C., Damste, J.S.S., Gottschal, J.C., Forney, L.J., Rouchy, J.M., 2002. CH4-consuming microorganisms and the formation of carbonate crusts at cold seeps. *Earth Planet. Sci. Lett.* **203**, 195–203.

Aloisi, G., Pierre, C., Rouchy, J.-M., Foucher, J.-P., Woodside, J., Party, T.M.S., 2000. Methane-related authigenic carbonates of eastern Mediterranean Sea mud volcanoes and their possible relation to gas hydrate destabilisation. *Earth Planet. Sci. Lett.* **184**, 321–338.

Barnes, R.O., Goldberg, E.D., 1976. Methane production and consumption in anoxic marine-sediments. *Geology* **4**, 297–300.

Berner, R.A., 1980. Early Diagenesis—a Theoretical Approach. Princeton University Press, Princeton, New Jersey.

Blumenberg, M., Seifert, R., Reitner, J., Pape, T., Michaelis, W., 2004. Membrane lipid patterns typify distinct anaerobic methanotrophic consortia. *Proc. Natl. Acad. Sci. USA*, 101.

Boetius, A., Ravenschlag, K., Schubert, C., Rickert, D., Widdel, F., Gieseke, A., Amann, R., Jørgensen, B.B., Witte, U., Pfannkuche, O., 2000. A marine microbial consortium apparently mediating anaerobic oxidation of methane. *Nature* **407**, 623–626.

Boetius, A., Suess, E., 2004. Hydrate Ridge: a natural laboratory for the study of microbial life fueled by methane from near-surface gas hydrates. *Chem. Geol.* **205**, 291–310.

Bohrmann, G., Ivanov, M., Foucher, J.P., Spiess, V., Bialas, J., Greinert, J., Weinrebe, W., Abegg, F., Aloisi, G., Artemov, Y., Blinova, V., Drews, M., Heidersdorf, F., Krabbenhoft, A., Klaucke, I., Krastel, S., Leder, T., Polikarpov, I., Saburova, M., Schmale, O., Seifert, R., Volkonskaya, A., Zillmer, M., 2003. Mud volcanoes and gas hydrates in the Black Sea: new data from Dvurechenskii and Odessa mud volcanoes. *Geo-Mar. Lett.* **23**, 239–249.

Boschker, H.T.S., Middelburg, J.J., 2002. Stable isotopes and biomarkers in microbial ecology. *FEMS Microbiol. Ecol.* **40**, 85–95.

Boudreau, B.P., 1997. Diagenetic Models and their Implementation: Modelling Transport and Reactions in Aquatic Sediments. Springer, Berlin.

Charlou, J.L., Donval, J.P., Zitter, T., Roy, N., Jean-Baptiste, P., Foucher, J.P., Woodside, J., 2003. Evidence of methane venting and geochemistry of brines on mud volcanoes of the eastern Mediterranean Sea. *Deep-Sea Res. Pt. I* **50**, 941–958.

Cita, M.B., Ryan, W.B.F., Paggi, L., 1981. Prometheus Mud Breccia: an example of shale diapirism in the western Mediterranean Ridge, Annales Ge'ologiques Des Pays Helle'niques.

Cline, J.D., 1969. Spectrophotometric Determination of Hydrogen Sulfide in Natural Waters. *Limnol. Oceanogr.* **14**, 454–458.

Cordes, E.E., Arthur, M.A., Shea, K., Arvidson, R.S., Fisher, C.R., 2005. Modeling the mutualistic interactions between tubeworms and microbial consortia. *Plos. Biol.* **3**, 497–506.

Damm, E., Budéus, G., 2003. Fate of vent-derived methane in seawater above the Hakon Mosby mud volcano (Norwegian Sea). *Mar. Chem.* **82**, 1–11.

Dando, P.R., Bussmann, I., Niven, S.J., O'hara, S.C.M., Schmaljohann, R., Taylor, L.J., 1994. A methane seep area in the Skagerrak, the habitat of the pogonophore Siboglinum poseidoni and the bivalve mollusc Thyasira sarsi. *Mar. Ecol-Prog. Ser.* **107**, 157–167.

De Beer, D., Sauter, E., Niemann, H., Kaul, N., Foucher, J.P., Witte, U., Schluter, M., Boetius, A., 2006. In situ fluxes and zonation of microbial activity in surface sediments of the Hakon Mosby Mud Volcano. *Limnol. Oceanogr.* **51**, 1315–1331.

Diaz-Del-Rio, V., Somoza, L., Martinez-Frias, J., Mata, M.P., Delgado, A., Hernandez-Molina, F.J., Lunar, R., Martin-Rubi, J.A., Maestro, A., Fernandez-Puga, M.C., Leon, R., Llave, E., Medialdea, T., Vazquez, J.T., 2003. Vast fields of hydrocarbon-derived carbonate chimneys related to the accretionary wedge/olistostrome of the Gulf of Cadiz. *Mar. Geol.* **195**, 177–200.

Dimitrov, L.I., 2002. Mud volcanoes—the most important pathway for degassing deeply buried sediments. *Earth-Sci. Rev.* **59**, 49–76.

Dimitrov, L.I., 2003. Mud volcanoes—a significant source of atmospheric methane. *Geo-Mar. Lett.* **23**, 155–161.

Elvert, M., Boetius, A., Knittel, K., Jorgensen, B.B., 2003. Characterization of specific membrane fatty acids as chemotaxonomic markers for sulfate-reducing bacteria involved in anaerobic oxidation of methane. *Geomicrobiol. J.* **20**, 403–419.

Elvert, M., Greinert, J., Suess, E., Whiticar, M.J., 2001. Carbon isotopes of biomarkers derived from methane-oxidizing microbes at hydrate ridge, Cascadia convergent margin. In: Paull, C.K., Dillon, W.P. (Eds.), *Natural Gas Hydrates: Occurrence, Distribution, and Dynamics*. American Geophysical Union, Washington DC.

Elvert, M., Hopmans, E.C., Treude, T., Boetius, A., Hinrichs, K.-U., 2005. Spatial variatons of archaeal-bacterial assambladges in gas hydrate bearing sediments at a cold seep: Implications from a high resolution molecular and isotopic approach. *Geobiology* **3**, 195–209.

Elvert, M., Suess, E., Whiticar, M.J., 1999. Anaerobic methane oxidation associated with marine gas hydrates: superlight C-isotopes from saturated and unsaturated C_{20} and C_{25} irregular isoprenoids. *Naturwissenschaften* **86**, 295–300.

Etiope, G., Klusman, R.W., 2002. Geologic emissions of methane to the atmosphere. *Chemosphere* **49**, 777–789.

Etiope, G., Milkov, A.V., 2004. A new estimate of global methane flux from onshore and shallow submarine mud volcanoes to the atmosphere. *Environ. Geol.* **46**, 997–1002.

Felbeck, H., 1983. Sulfide oxidation and carbon fixation by the gutless clam solemya-reidi—an animal bacteria symbiosis. *J. Comp. Physiol.* **152**, 3–11.

Fisher, C.R., 1990. Chemoautotrophic and methanotrophic symbioses in marine-invertebrates. *Rev. Aquat. Sci.* **2**, 399–436.

Gardner, J.M., 2001. Mud volcanoes revealed and sampled on the Western Moroccan continental margin. *Geophys. Res. Lett.* **28**, 339–342.

Gebruk, A.V., Krylova, E.M., Lein, A.Y., Vinogradov, G.M., Anderson, E., Pimenov, N.V., Cherkashev, G.A., Crane, K., 2003. Methane seep community of the Hakon Mosby mud volcano (the Norwegian Sea): composition and trophic aspects. *Sarsia* **88**, 394–403.

Gillian, F.T., Johns, R.B., Verheyen, T.V., Nichols, P.D., Esdaile, R.J., Bavor, H.J., 1981. Monounsaturated fatty acids as specific bacterial markers in marine sediments. *Adv. Org. Geochem.*.

Grasshoff, K., Ehrhardt, M., Kremling, K., 1983. *Methods of seawater analysis*. Verlag Chemie, Weinheim.

Haese, R.R., Meile, C., Van Cappellen, P., De Lange, G.J., 2003. Carbon geochemistry of cold seeps: methane fluxes and transformation in sediments from Kazan mud volcano, eastern Mediterranean Sea. *Earth Planet. Sci. Lett.* **212**, 361–375.

Hanson, R.S., Hanson, T.E., 1996. Methanotrophic bacteria. *Microbiol. Rev.* **60**, 439.

Hensen, C., Wallmann, K., Schmidt, M., Ranero, C.R., Suess, E., 2004. Fluid expulsion related to mud extrusion off Costa Rica—a window to the subducting slab. *Geology* **32**, 201–204.

Hensen, C., Zabel, M., Pfeifer, K., Schwenk, T., Kasten, S., Riedinger, N., Schulz, H.D., Boettius, A., 2003. Control of sulfate pore-water profiles by sedimentary events and the significance of anaerobic oxidation of methane for the burial of sulfur in marine sediments. *Geochim. Cosmochim. Acta* **67**, 2631–2647.

Hinrichs, K.-U., Boetius, A., 2002. The anaerobic oxidation of methane: new insights in microbial ecology and biogeochemistry. In: Wefer, G., Billett, D., Hebbeln, D. (Eds.), *Ocean Margin System*. Springer-Verlag, Berlin.

Hinrichs, K.-U., Hayes, J.M., Sylva, S.P., Brewer, P.G., Delong, E.F., 1999. Methane-consuming archaebacteria in marine sediments. *Nature* **398**, 802–805.

Iversen, N., Jørgensen, B.B., 1985. Anaerobic methane oxidation rates at the sulfate–methane transition in marine sediments from Kattegat and Skagerrak (Denmark). *Limnol. Oceanogr.* **30**, 944–955.

Jørgensen, B.B., 1978. A comparison of methods for the quantification of bacterial sulphate reduction in coastal marine sediments. I. Measurements with radiotracer techniques. *Geomicrobiol. J.* **1**, 11–27.

Jørgensen, B.B., Weber, A., Zopfi, J., 2001. Sulfate reduction and anaerobic methane oxidation in Black Sea sediments. *Deep-Sea Res. Pt. I* **48**, 2097–2120.

Joye, S.B., Boetius, A., Orcutt, B.N., Montoya, J.P., Schulz, H.N., Erickson, M.J., Lugo, S.K., 2004. The anaerobic oxidation of methane and sulfate reduction in sediments from Gulf of Mexico cold seeps. *Chem. Geol.* **205**, 219–238.

Judd, A.G., Hovland, M., Dimitrov, L.I., Gil, S.G., Jukes, V., 2002. The geological methane budget at continental margins and its influence on climate change. *Geofluids* **2**, 109–126.

Kane, M.D., Poulsen, L.K., Stahl, D.A., 1993. Monitoring the enrichment and isolation of sulfate-reducing bacteria by using oligonucleotide hybridization probes designed from environmentally derived 16s ribosomal-Rna sequences. *Appl. Environ. Microbiol.* **59**, 682–686.

Kenyon, N.H., Ivanov, M.K., Akhmetzhanov, A.M., Akhmanov, G., 2001. Interdisciplinary Approaches to Geoscience on the North East Atlantic Margin and Mid-Atlantic Ridge. IOC Technical Series No. 60.

Kenyon, N.H., Ivanov, M.K., Akhmetzhanov, A.M., Akhmanov, G.G., 2000. Multidisciplinary Study of Geological Processes on the North

East Atlantic and Western Mediterranean Margins. IOC Technical Series No. 56.

Kholodov, V.N., 2002. Mud volcanoes: distribution regularities and genesis (Communication 2. geological–geochemical peculiarities and formation model). *Lithol. Miner. Resour.* **37**, 293–310.

Kimura, H., Sato, M., Sasayama, Y., Naganuma, T., 2003. Molecular characterization and in situ localization of endosymbiotic 16S ribosomal RNA and RuBisCO genes in the pogonophoran tissue. *Mar. Biotechnol.* **5**, 261–269.

Knittel, K., Boetius, A., Lemke, A., Eilers, H., Lochte, K., Pfannkuche, O., Linke, P., Amann, R., 2003. Activity, distribution, and diversity of sulfate reducers and other bacteria in sediments above gas hydrate (Cascadia margin, Oregon). *Geomicrobiol. J.* **20**, 269–294.

Knittel, K., Lösekann, T., Boetius, A., Kort, R., Amann, R., 2005. Diversity and distribution of methanotrophic archaea at cold seeps. *Appl. Environ. Microbiol.* **71**, 467–479.

Kopf, A., Bannert, B., Brückmann, W., Dorschel, B., Foubert, A.T.G., Grevemeyer, I., Gutscher, M.A., Hebbeln, D., Heesemann, B., Hensen, C., Kaul, N.E., Lutz, M., Magalhaes, V.H., Marquardt, M.J., Marti, A.V., Nass, K.S., Neubert, N., Niemann, H., Nuzzo, M., Poort, J.P.D., Rosiak, U.D., Sahling, H., Schneider Von Deimling, J., Somoza, L., Thiebot, E., Wilkop, T.P., 2004. Report and preliminary results of Sonne Cruise SO175, Miami–Bremerhaven, 12.11—30.12.2003. Fachbereich Geowissenschaften der Universität Bremen.

Kopf, A.J., 2002. Significance of mud volcanism. *Rev. Geophys.* **40**, B1–B49.

Kopf, A.J., 2003. Global methane emission through mud volcanoes and its past and present impact on the Earth's climate. *Int. J. Earth Sci.* **92**, 806–816.

Krueger, D.M., Cavanaugh, C.M., 1997. Phylogenetic diversity of bacterial symbionts of Solemya hosts based on comparative sequence analysis of 16S rRNA genes. *Appl. Environ. Microbiol.* **63**, 91–98.

Lane, D.J., Pace, B., Olsen, G.J., Stahl, D.A., Sogin, M.L., Pace, N.R., 1985. Rapid-determination of 16s ribosomal-Rna sequences for phylogenetic analyses. *Proc. Natl. Acad. Sci. USA* **82**, 6955–6959.

Luff, R., Wallmann, K., 2003. Fluid flow, methane fluxes, carbonate precipitation and biogeochemical turnover in gas hydrate-bearing sediments at hydrate ridge, Cascadia margin: numerical modeling and mass balances. *Geochim. Cosmochim. Acta* **67**, 3403–3421.

Madigan, M.T., Martinko, J.M., Parker, J., 2000. *Brock Biology of Microorganisms*. Prentice-Hall Inc..

Maldonado, A., Comas, M.C., 1992. Geology and geophysics of the Alboran Sea—an introduction. *Geo-Mar. Lett.* **12**, 61–65.

Maldonado, A., Somoza, L., Pallares, L., 1999. The Betic orogen and the Iberian–African boundary in the Gulf of Cadiz: geological evolution (central North Atlantic). *Mar. Geol.* **155**, 9–43.

Massana, R., Murray, A.E., Preston, C.M., Delong, E.F., 1997. Vertical distribution and phylogenetic characterization of marine planktonic Archaea in the Santa Barbara Channel. *Appl. Environ. Microbiol.* **63**, 50–56.

Mazurenko, L.L., Soloviev, V.A., Belenkaya, I., Ivanov, M.K., Pinheiro, L.M., 2002. Mud volcano gas hydrates in the Gulf of Cadiz. *Terra Nova* **14**, 321–329.

Michaelis, W., Seifert, R., Nauhaus, K., Treude, T., Thiel, V., Blumenberg, M., Knittel, K., Gieseke, A., Peterknecht, K., Pape, T., Boetius, A., Amann, R., Jorgensen, B.B., Widdel, F., Peckmann, J.R., Pimenov, N.V., Gulin, M.B., 2002. Microbial reefs in the Black Sea fueled by anaerobic oxidation of methane. *Science* **297**, 1013–1015.

Milkov, A.V., 2000. Worldwide distribution of submarine mud volcanoes and associated gas hydrates. *Mar. Geol.* **167**, 29–42.

Milkov, A.V., Sassen, R., Apanasovich, T.V., Dadashev, F.G., 2003. Global gas flux from mud volcanoes: a significant source of fossil methane in the atmosphere and the ocean. *Geophys. Res. Lett.*, 30.

Milkov, A.V., Vogt, P.R., Crane, K., Lein, A.Y., Sassen, R., Cherkashev, G.A., 2004. Geological, geochemical, and microbial processes at the hydrate-bearing Hakon Mosby mud volcano: a review. *Chem. Geol.* **205**, 347–366.

Moss, C.W., Lambertfair, M.A., 1989. Location of double-bonds in monounsaturated fatty-acids of campylobacter-cryaerophila with dimethyl disulfide derivatives and combined gas chromatography-mass spectrometry. *J. Clin. Microbiol.* **27**, 1467–1470.

Muyzer, G., Teske, A., Wirsen, C.O., Jannasch, H.W., 1995. Phylogenetic relationships of Thiomicrospira species and their identification in deep-sea hydrothermal vent samples by denaturing gradient gel electrophoresis of 16S rDNA fragments. *Arch. Microbiol.* **164**, 165–172.

Nauhaus, K., Boetius, A., Kruger, M., Widdel, F., 2002. In vitro demonstration of anaerobic oxidation of methane coupled to sulphate reduction in sediment from a marine gas hydrate area. *Environ. Microbiol.* **4**, 296–305.

Nichols, P.D., Guckert, J.B., White, D.C., 1986. Determination of monounsaturated fatty acid double-bond position and geometry for microbial monocultures and complex consortia by capillary GC-MS of their dimethyl disulphide adducts. *J. Microbiol. Methods* **5**, 49–55.

Niemann, H., Elvert, M., Hovland, M., Orcutt, B., Judd, A.G., Suck, I., Gutt, J., Joye, S.B., Damm, E., Finster, K., Boetius, A., 2005. Methane emission and consumption at a North Sea gas seep (Tommeliten area). *Biogeosciences* **2**, 335–351.

Niewöhner, C., Hensen, C., Kasten, S., Zabel, M., Schulz, H.D., 1998. Deep sulfate reduction completely mediated by anaerobic methane oxidation in sediments of the upwelling area off Namibia. *Geochim. Cosmochim. Acta* **62**, 455–464.

Nuzzo, M., Hensen, C., Hornibrook, E., Brueckmann, W., Magalhaes, V.H., Parkes, R.J., Pinheiro, L.M., 2005. Origin of Mud Volcano Fluids in the Gulf of Cadiz (E-Atlantic) EGU General Assembly, Vienna.

Olu, K., Lance, S., Sibuet, M., Henry, P., Fialamedioni, A., Dinet, A., 1997a. Cold seep communities as indicators of fluid expulsion patterns through mud volcanoes seaward of the Barbados accretionary prism. *Deep-Sea Res. Pt. I* **44**, 811.

Olu, K., Lance, S., Sibuet, M., Henry, P., Fiala-Médioni, A., Dinet, A., 1997b. Cold seep communities as indicators of fluid expulsion patterns through mud volcanoes seaward of the Barbados accretionary prism. *Deep-Sea Res. I* **44**, 811–841.

Orphan, V.J., House, C.H., Hinrichs, K.U., Mckeegan, K.D., Delong, E.F., 2001. Methane-consuming archaea revealed by directly coupled isotopic and phylogenetic analysis. *Science* **293**, 484–487.

Orphan, V.J., House, C.H., Hinrichs, K.U., Mckeegan, K.D., Delong, E.F., 2002. Multiple archaeal groups mediate methane oxidation in anoxic cold seep sediments. *Proc. Natl. Acad. Sci. USA* **99**, 7663–7668.

Pancost, R.D., Bouloubassi, I., Aloisi, G., Damste, J.S.S., 2001. Three series of non-isoprenoidal dialkyl glycerol diethers in cold-seep carbonate crusts. *Org. Geochem.* **32**, 695–707.

Pancost, R.D., Sinninghe Damsté, J.S., De Lint, S., Van Der Maarel, M.J.E.C., Gottschal, J.C., Party, T.M.S.S., 2000. Biomarker evidence for widespread anaerobic methane oxidation in Mediterranean sediments by a consortium of methanogenic archaea and bacteria. *Appl. Environ. Microbiol.* **66**, 1126–1132.

Peckmann, J., Thiel, V., Michaelis, W., Clari, P., Gaillard, C., Martire, L., Reitner, J., 1999. Cold seep deposits of Beauvoisin (Oxfordian; southeastern France) and Marmorito (Miocene; northern Italy): microbially induced authigenic carbonates. *Int. J. Earth Sci.* **88**, 60–75.

Peek, A.S., Feldman, R.A., Lutz, R.A., Vrijenhoek, R.C., 1998. Cospeciation of chemoautotrophic bacteria and deep sea clams. *Proc. Natl. Acad. Sci. USA* **95**, 9962–9966.

Pinheiro, L.M., Ivanov, M.K., Sautkin, A., Akhmanov, G., Magalhaes, V.H., Volkonskaya, A., Monteiro, J.H., Somoza, L., Gardner, J., Hamouni, N., Cunha, M.R., 2003. Mud volcanism in the Gulf of Cadiz: results from the TTR-10 cruise. *Mar. Geol.* **195**, 131–151.

Reeburgh, W.S., 1967. An improved interstitial water sampler. *Limnol. Oceanogr.* **12**, 163.

Reeburgh, W.S., 1976. Methane consumption in Cariaco Trench waters and sediments. *Earth Planet. Sci. Lett.* **28**, 337–344.

Reeburgh, W.S., 1996. "Soft spots" in the global methane budget. In: Lidstrom, M.E., Tabita, F.R. (Eds.), *Microbial Growth on C_1 Compounds*. Kluwer Academic Publishers, Dordrecht.

Reeburgh, W.S., Heggie, D.T., 1977. Microbial methane consumption reactions and their effect on methane distributions in freshwater and marine environments. *Limnol. Oceanogr.* **22**, 1–9.

Ritger, S., Carson, B., Suess, E., 1987. Methane-derived authigenic carbonates formed by subduction-induced pore-water expulsion along the Oregon/Washington margin. *Geol. Soc. Am. Bull.* **98**, 147–156.

Rueter, P., Rabus, R., Wilkes, H., Aeckersberg, F., Rainey, F.A., Jannasch, H.W., Widdel, F., 1994. Anaerobic oxidation of hydrocarbons in crude-oil by new types of sulfate-reducing bacteria. *Nature* **372**, 455–458.

Sahling, H., Rickert, D., Lee, R.W., Linke, P., Suess, E., 2002. Macrofaunal community structure and sulfide flux at gas hydrate deposits from the Cascadia convergent margin, NE Pacific. *Mar. Ecol-Prog. Ser.* **231**, 121–138.

Sauter, E.J., Muyakshin, S.I., Charlou, J.-L., Schluter, M., Boetius, A., Jerosch, K., Damm, E., Foucher, J.-P., Klages, M., 2006. Methane discharge from a deep-sea submarine mud volcano into the upper water column by gas hydrate-coated methane bubbles. *Earth Planet. Sci. Lett.* **243**, 354–365.

Schmaljohann, R., Flugel, H.J., 1987. Methane-oxidizing bacteria in pogonophora. *Sarsia* **72**, 91–99.

Sibuet, M., Olu, K., 1998. Biogeography, biodiversity and fluid dependence of deep-sea cold-seep communities at active and passive margins. *Deep-Sea Res. Pt. II* **45**, 517–567.

Small, H., Stevens, T.S., Bauman, W.C., 1975. Novel ion-exchange chromatographic method using conductimetric detection. *Anal. Chem.* **47**, 1801–1809.

Somoza, L., Diaz-Del-Rio, V., Leon, R., Ivanov, M., Fernandez-Puga, M.C., Gardner, J.M., Hernandez-Molina, F.J., Pinheiro, L.M., Rodero, J., Lobato, A., Maestro, A., Vazquez, J.T., Medialdea, T., Fernandez-Salas, L.M., 2003. Seabed morphology and hydrocarbon seepage in the Gulf of Cadiz mud volcano area: Acoustic imagery, multibeam and ultra-high resolution seismic data. *Mar. Geol.* **195**, 153–176.

Somoza, L., Diaz-Del-Rio, V., Vaszquez, J.T., Pinheiro, L.M., Hernandez-Molina, F.J., 2002. Numerous methane gas-related sea floor structures identified in Gulf of Cadiz. *EOS* **83**, 541–547.

Southward, A.J., Southward, E.C., Dando, P.R., Barrett, R.L., Ling, R., 1986. Chemoautotrophic function of bacterial symbionts in small pogonophora. *J. Mar. Biol. Assoc. UK* **66**, 415–437.

Southward, A.J., Southward, E.C., Dando, P.R., Rau, G.H., Felbeck, H., Fluegel, H., 1981. Bacterial symbionts and low $^{13}C/^{12}C$ ratios in tissues of Pogonophora indicate unusual nutrition and metabolism. *Nature* **293**, 616–620.

Southward, E.C., Schulze, A., Gardiner, S.L., 2005. Pogonophora (Annelida): form and function. *Hydrobiologia* **535–536**, 227–251.

Stadnitskaia, A., Ivanov, M.K., Blinova, V., Kreulen, R., Van Weering, T.C.E., 2006. Molecular and carbon isotopic variability of hydrocarbon gases from mud volcanoes in the Gulf of Cadiz, NE Atlantic. *Mar. Petrol. Geol.* **23**, 281–296.

Stadnitskaia, A., Muyzer, G., Abbas, B., Coolen, M.J.L., Hopmans, E.C., Baas, M., Van Weering, T.C.E., Ivanov, M.K., Poludetkina, E., Damste, 2005. Biomarker and 16S rDNA evidence for anaerobic oxidation of methane and related carbonate precipitation in deep-sea mud volcanoes of the Sorokin Trough, Black Sea. *Mar. Geol.* **217**, 67–96.

Summons, R.E., Jahnke, L.L., Roksandic, Z., 1994. Carbon isotopic fractionation in lipids from methanotrophic bacteria: relevance for interpretation of the geochemical record of biomarkers. *Geochim. Cosmochim. Acta* **58**, 2853–2863.

Teske, A., Hinrichs, K.U., Edgcomb, V., Gomez, A.D., Kysela, D., Sylva, S.P., Sogin, M.L., Jannasch, H.W., 2002. Microbial diversity of hydrothermal sediments in the Guaymas basin: evidence for anaerobic methanotrophic communities. *Appl. Environ. Microbiol.* **68**, 1994–2007.

Thiel, V., Peckmann, J., Seifert, R., Wehrung, P., Reitner, J., Michaelis, W., 1999. Highly isotopically depleted isoprenoids: molecular markers for ancient methane venting. *Geochim. Cosmochim. Acta* **63**, 3959–3966.

Torres, M.E., Mcmanus, J., Hammond, D.E., De Angelis, M.A., Heeschen, K.U., Colbert, S.L., Tryon, M.D., Brown, K.M., Suess, E., 2002. Fluid and chemical fluxes in and out of sediments hosting methane hydrate deposits on hydrate ridge, OR, I: hydrological provinces. *Earth Planet. Sci. Lett.* **201**, 525–540.

Treude, T., Boetius, A., Knittel, K., Wallmann, K., Jorgensen, B.B., 2003. Anaerobic oxidation of methane above gas hydrates at hydrate ridge, NE Pacific Ocean. *Mar. Ecol-Prog. Ser.* **264**, 1–14.

Treude, T., Niggemann, J., Kallmeyer, J., Wintersteller, P., Schubert, C.J., Boetius, A., Jorgensen, B.B., 2005. Anaerobic oxidation of methane and sulfate reduction along the Chilean continental margin. *Geochim. Cosmochim. Acta* **69**, 2767–2779.

Vogt, P.R., Cherkashev, A., Ginsburg, G.D., Ivanov, G.I., Crane, K., Lein, A.Y., Sundvor, E., Pimenov, N.V., Egorov, A., 1997a. Haakon mosby mud volcano: a warm methane seep with seafloor hydrates and chemosynthesis-based ecosystem in late quantemary slide valley, Bear Island Fan, Barents Sea passive margin. *EOS Trans. Am. Geophys. Union Suppl.* **78**, 187–189.

Vogt, P.R., Cherkashev, G., Ginsburg, G., Ivanov, G.I., Milkov, A., Crane, K., Lein, A., Sundvor, E., Pimenov, N.V., Egorov, A., 1997b. Haakon mosby mud volcano provides unusual example of venting. *EOS Trans. Am. Geophys. Union Suppl.* **78** (549), 556–557.

Werne, J.P., Baas, M., Damste, J.S.S., 2002. Molecular isotopic tracing of carbon flow and trophic relationships in a methane-supported benthic microbial community. *Limnol. Oceanogr.* **47**, 1694–1701.

Werne, J.P., Haese, R.R., Zitter, T., Aloisi, G., Bouloubassi, L., Heijs, S., Fiala-Medioni, A., Pancost, R.D., Damste, J.S.S., De Lange, G., Forney, L.J., Gottschal, J.C., Foucher, J.P., Mascle, J., Woodside, J., 2004. Life at cold seeps: a synthesis of biogeochemical and ecological data from Kazan mud volcano, eastern Mediterranean Sea. *Chem. Geol.* **205**, 367–390.

Whiticar, M.J., 1999. Carbon and hydrogen isotope systematics of bacterial formation and oxidation of methane. *Chem. Geol.* **161**, 291–314.

Whiticar, M.J., Faber, E., Schoell, M., 1986. Biogenic methane formation in marine and freshwater environments: CO_2 reduction vs. acetate fermentation—isotope evidence. *Geochim. Cosmochim. Acta* **50**, 693–709.

Widdel, F., Rabus, R., 2001. Anaerobic biodegradation of saturated and aromatic hydrocarbons. *Curr. Opin. Biotechnol.* **12**, 259–276.